Communications Subsystem Test Bench and Design Verification for Foresail-1 CubeSat

Ville-Valtteri Kettunen

School of Electrical Engineering

Thesis submitted for examination for the degree of Master of Science in Technology.

Espoo 22.11.2021

Supervisor and advisor

Assistant Prof. Jaan Praks

Aalto University
School of Electrical
Engineering

Aalto University
School of Electrical
Engineering

Aalto University, P.O. BOX 11000, 00076 AALTO
www.aalto.fi
Abstract of the master's thesis

Author Ville-Valtteri Kettunen

Title Communications Subsystem Test Bench and Design Verification for Foresail-1 CubeSat

Degree programme Electronics and Nanotechnology

Major Microwave Engineering **Code of major** ELEC3051

Supervisor and advisor Assistant Prof. Jaan Praks

Date 22.11.2021 **Number of pages** 90+1 **Language** English

Abstract

Nanosatellites, with weight less than 10 kg have become very popular with the help of the CubeSat standard, low launch prices and usage of cheaper electronic components. Many new countries have launched their first satellite in this category. Educational institutions and amateurs have been able to build and launch satellites with limited resources, and many new companies use nanosatellites to provide new services. Unfortunately, the rapid development times and inexperienced teams brings up a problem with reliability. Many satellites in this category never make contact to a ground station and are congesting the low Earth orbits as space junk. The aim of this thesis is to create a framework for CubeSat communications subsystem testing. In this work, a test bench is created from current methods in the CubeSat testing practices, as well as industry level standardized tests. The tests are applied to the Foresail-1 satellite communications subsystem development. A part of successful testing is a good design and therefore, a part of the thesis is dedicated to simulating and implementing matching circuits and filters to radio frequency signal paths of the mentioned satellite. Proper filter design and impedance matching ensures high efficiency for the transmit side and a high sensitivity for the receive side. The test benches are used to confirm that the Foresail-1 communications subsystem not only meets the requirements set to the system by the mission, but the requirements set by the regulation from the International Telecommunications Union. Additionally important aspects such as the Doppler shift is considered. The developed approach is documented, and it can be adapted to future CubeSat projects.

Keywords Foresail, COM , nanosatellite , CubeSat, testing , communications

Aalto University
School of Electrical
Engineering

Aalto-yliopisto, PL 11000, 00076 AALTO
www.aalto.fi
Diplomityön tiivistelmä

Tekijä Ville-Valtteri Kettunen

Työn nimi Foresail-1 CubeSat satelliitin radiokommunikaatiojärjestelmän testialusta ja järjestelmän verifiointi

Koulutusohjelma Elektroniikan ja nanotekniikan laitos

Pääaine Mikroaaltotekniikka **Pääaineen koodi** ELEC3051

Työn valvoja ja ohjaaja Assistant Prof. Jaan Praks

Päivämäärä 22.11.2021 **Sivumäärä** 90+1 **Kieli** Englanti

Tiivistelmä

Nanosatelliitit, joiden massa on alle 10 kg, ovat yleistyneet CubeSat-standardin myötä. Standardi on mahdollistanut edullisemmat laukaisut ja tavallisten elektroniikan komponenttien käytön satelliiteissa. Monet maat ovat lähettäneet ensimmäiset satelliittinsa tässä satelliittiluokassa. Koulutuslaitokset ja amatöörit ovat pystyneet rakentamaan ja lähettämään satelliitteja matalilla resursseillaan, ja monet uudet yritykset käyttävät nanosatelliitteja uusien palveluiden tuottamiseen. Valitettavasti nopeat kehitysaikataulut ja kokemattomuus ovat tuoneet mukanaan luotettavuuteen liittyviä ongelmia. Monet satelliitit tässä kategoriassa eivät laukaisunsa jälkeen saa enää yhteyttä maa-asemaansa. Tämä johtaa siihen, että satelliiteista tulee avaruusromua. Tämän työn tarkoituksena on luoda CubeSat kommunikaatiojärjestelmän testausjärjestely. Tässä työssä tehdään testausjärjestelmä, jossa hyödynnetään nykyisin käytössä olevia CubeSat testaustapoja ja teollisuuden standardeihin perustuvia testitapoja. Testausta sovelletaan Foresail-1 satelliitin kommunikaatioalijärjestelmän kehitykseen. Osa onnistunutta testikampanjaa liittyy hyvään suunnitteluun. Tästä syystä osa tästä työstä keskittyy radiotaajuuspiirien suunnittelutyökaluihin ja mittaukseen, joiden avulla sovituspiirejä ja radiotaajuussuodattimien toiminta varmistetaan. Hyvät suodattimet ja sovituspiirit takaavat signaalin lähetyspuolella hyvän hyötysuhteen, ja vastaanottopuolella hyvän herkkyyden. Lopulta testataan Foresail-1 satelliitin kommunikaatiojärjestelmän toiminta, ja varmistetaan että toimintakyky vastaa satelliitille sen tehtävän asettamia vaatimuksia. Testeillä varmistetaan myös toiminnan noudattavan kansainvälisten radiotaajuuskäyttöä valvovien sopimusten asettamia rajoja. Lisäksi testataan satelliittijärjestelmälle tärkeitä parametreja, kuten Doppler siirtymän vaikutus radion vastaanottokykyyn. Kehitetty testijärjestely on dokumentoitu työssä, ja sitä voidaan soveltaa tuleviin nanosatelliittiprojekteihin.

Avainsanat CubeSat, nanosatelliitti, radiojärjestelmä, testaaminen, Foresail, COM

Contents

Symbols

$\frac{S}{N}$	signal to noise ratio
E_b	energy per bit
N_0	nose power spectral density
f_b	data rate
B	bandwidth
P_r	received power
P_t	transmitted power
G_t	gain of transmitting antenna
G_r	gain of receiving antenna
λ	wavelength
R	distance
L_s	free space path loss
f	frequency
B_T	transmission bandwidth
OBW	occupied bandwidth
B_n	necessary bandwidth
D	frequency deviation
S	number of signalling states
β_f	frequency modulation index
ΔF	frequency deviation
Z_0	characteristic impedance
d	thickness
w	width
η	intrinsic impedance of a dielectric medium
μ	peameability
ϵ	absolute permittivity
Z_L	load impedance
Γ	reflection coefficient
T	transmission coefficient
IL	insertion loss
RL	return loss
S_{ij}	S-parameter from port j to i
V_i^-	voltage wave moving into negative direction at port i
V_i^+	voltage wave moving into positive direction at port i
Pn	Noise power
k	Boltzmann constant
T	Temperature
L	loss
f_m	doppler shift
c	speed of light
f_c	carrier frequency

Abbreviations

ADC	Analog-to-Digital converter
ADCS	Attitude Determination and Control System
ASK	Amplitude Shift Keying
BFSK	Binary Frequency Shift Keying
CDS	CubeSat Design Specification
COM	Radio communications subsystem
COTS	Commercial Off-The-Shelf
CST	CST Studio software
DOA	Dead On Arrival
EPS	Electric Power System
ESA	European Space Agency
ETSI	European Telecommunications Standards Institute
FMI	Finnish Meteorological Institute
FSK	Frequency Shift Keying
FSPL	Free Space Path Loss
GMSK	Gaussian Minimum Shift Keying
IARU	International Amateur Radio Union
IC	Integrated Circuit
ITU	International Telecommunications Union
MEMS	Micro-electromechanical System
MSK	Minimum Shift Keying
NASA	The National Aeronautics and Space Administration
OBC	On-Board Computer
OCW	Operating Channel Bandwidth
PATE	Particle Telescope
PB	Plasma Break
PLL	Phase Locked Loop
PSK	Phase Shift Keying
QUCS	Quite Universal Circuit Simulator
SNR	Signal-to-Noise Ratio
SRD	Short Range Device
SWR	Standing Wave Ratio
TCXO	Thermal Compensated Crystal Oscillator
TDD	Time Division Duplexing
U	Unit of CubeSat, 10x10x10 cm cube
VNA	Vector Network Analyzer
WRC-19	World Radiocommunication Conference 2019

1 Introduction

Nanosatellites are satellites that have a mass between 1 and 10 kilograms. The development of the CubeSat standard in 1999 helped make number of nanosatellites in low Earth orbit grow significantly in the past two decades [25]. CubeSat nanosatellites have gained popularity as a cost-efficient way for amateurs, educational institutions, and corporations to do experimentation in Earth orbit [64]. Aalto University is involved in building a 8 kg CubeSat nanosatellite, Foresail-1, which is to be launched to the low Earth orbit. The radio frequency communication system of the satellite functions as the method of communication between the ground station located at Aalto campus area in Espoo and the satellite. The communications subsystem is custom built at Aalto for this mission, and uses common off-the-shelf components in its design.

A CubeSat communication subsystem often uses a radio with a coordinated frequency in the amateur radio band or a commercial band, and is always required to follow the regulations and recommendations concerning the use of the radio frequency spectrum laid out by the International Telecommunications Union (ITU) [68]. However, as typical CubeSat project does not have the resources to perform costly third party radio frequency compliance testing, and as it is not required, the burden of testing for compliance is on the CubeSat team. Unfortunately, many CubeSat projects do not have enough time, resources, or expertise to perform a thorough enough testing scheme to cover compliance testing, which can lead to mission failure. [43]

An in-house built CubeSat communications subsystems is often built from commercial off-the-shelf components, instead of expensive space-grade high reliability components [64]. When designing a new radio frequency circuit board, the design cannot be simply copied from a manufacturer supplied development board or off a datasheet. This is because the supporting circuitry, specific operating to frequency, or the design of the layout are usually different. A radio frequency design is sensitive to the layout of the tracks and components on the circuit board, as well as lumped element component values. Therefore, simulations, component level testing and ultimately an iterative process of component selection are typically required to ensure good functionality and efficiency of the radio subsystem.

There exist industry standards for radio frequency devices that could be applicable to the testing of a CubeSat communications subsystem. One organization which publishes standards for testing is the European Cooperation for Space Standardization (ECSS) [63]. The ECSS is supported by the European Space Agency. Another is the European Telecommunications Standards Institute (ETSI), specifically focusing on microwave devices. Ultimately the rules and limits for microwave transmissions are given in the ITU recommendations and rules. However for a team building a CubeSat, this information can be difficult to find and apply in the product development. Therefore, the aim of this thesis is to create a framework for CubeSat communications systems design verification and testing, and the application of the methods on the Foresail-1 CubeSat UHF Communications system built at Aalto University. To accomplish this task, this thesis will develop a test bench, which includes applicable

tests found in standards and typical documented CubeSat communications subsystem tests. The Foresail-1 communications subsystem is tested using this test bench, and the results are assessed to confirm the correct performance of the subsystem. Additionally, tools and methods for radio frequency tuning and matching are utilized to improve the radio frequency portion design of the system.

The rest of the thesis is divided into five chapters. Chapter 2 works as an introduction to the CubeSat communications subsystems, reviews applicable testing standards and commonly performed tests on CubeSat communications systems as well as gives some relevant theoretical background to microwave communications. Chapter 3 describes the partial redesign and implementation phases that were needed in order to improve the Foresail-1 communications subsystem initial design. Chapter 4 introduces the test plan and describes the testing phase by detailing the test setup and test results. Chapter 5 concludes the thesis by discussing the applicability of the designed test bench and the obtained results and suggesting future work.

2 Nanosatellite radio communications

Nanosatellites are a class of satellites that weigh between 1 and 10 kg. [23] The success of nanosatellites in the modern space era was enabled by the creation of the CubeSat standard in 1999 [2]. The growing number of satellites in orbit brings also challenges. Both orbits and the microwave spectrum are finite resources. ITU has the responsibility to govern over the use of the microwave spectrum, and operates under international agreements [68].

The reader of this thesis should understand that the word nanosatellite is almost synonymous with the word CubeSat nowadays because of the overwhelming majority of nanosatellites being CubeSats. For this reason, in parts this thesis also uses the word CubeSat in cases where it could be generalized to all nanosatellites, and even all satellites in general. It is noted by ITU that when it comes to orbits and microwave spectrum use, the weight of the satellite is of no significance. The important parameters involve how much power and bandwidth the transmitter of the satellite uses and into what direction is it radiating. [68]

2.1 CubeSat nanosatellites

CubeSat's are a subset of nanosatellites that follow the specifications laid out by the CubeSat Design Specification (CDS) document. The specification was created in California Polytechnic State University in 1999. It defines a standardized structure size and form for the satellite, measured in units of 10 by 10 by 10 cm cubes (unit, U). The standard form factor enables the use of standard sized CubeSat dispenser which is used by the launch vehicle to deploy the CubeSats into orbit. [2] Today over 1000 operational CubeSats have been launched into orbit, with the majority of them being 3U sized [41].

2.1.1 Frequencies utilized by CubeSats

Many CubeSats operate on specified radio bands allocated for amateur radio use in space by the International Amateur Radio Union (IARU), mainly in the 2-meter VHF band from 145.794 MHz to 146 MHz, and the 70-centimeter UHF band from 435 MHz - 438 MHz. The typical maximum baud rate of CubeSats in the mentioned amateur radio bands is 9600, which sets a limit to the amount of data the satellite can downlink daily. the 2 GHz band is also sometimes utilized for this reason in either in the industrial, scientific and medical (ISM) or commercial bands, allowing data rates in the hundreds of kilobits per second. The main problem using the ISM bands is the congestion and noise generated by appliances and wireless systems, leading to interference and an overall higher noise floor. [24]

Higher frequencies allow for higher data rates because of more available bandwidth. The higher data rates become necessary as more data is generated by more capable payloads. As the increase of required data rate mostly concerns the downlink, increasing only the satellite transmit frequency is required. Experimentation in the Ka-band at 26.8 GHz has been shown to provide data rates of up to 320 Mbps,

enabling over 10 GB of data downlinked per satellite pass. [44], [72]. One example of a commercial X-band transmitter, operating at 7.9 - 8.4 GHz frequency, is an Endurosat X-band transmitter which is capable of 124 Mbps data rates according to their datasheet [13]. This also shows the X-band has moved from an experimental into a clearly commercial area.

Today the X-band has already become the third most common downlink band according to an unofficial database consisting of 3200 nanosatellites. The UHF frequencies are still clearly in the lead when it comes to overall numbers. The statistics for downlink frequencies used by nanosatellites according to nanosats.eu is shown in Figure 1 [41].

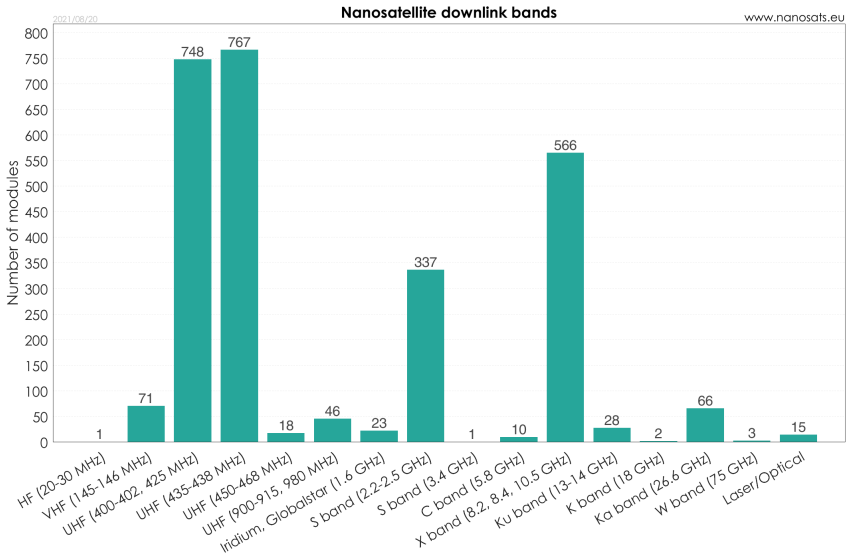

Figure 1: Nanosatellite downlink frequency statistics from a database collected by nanosats.eu. Situation in 20.8.2021. The UHF band is equally common in the commercial and amateur frequencies. [41]

When it comes to the amateur radio frequencies in the UHF band, IARU publishes a list of satellite projects for which they have coordinated frequencies. Data scraped from this list shows that a fairly narrow band of the allocated amateur satellite spectrum is actually popular for satellite coordination by IARU. The data scraped from the www.amsatuk.me.uk/iaru/finished.php published list of satellites is shown in Figure 2.

The coordination of a frequency does not mean you own that frequency band. For example over 25 different satellites have been coordinated to the frequency 437.325 MHz. It is clear that the amateur radio frequencies are a shared resource, and users have to accept some possibility of interference from other satellites and users of the bands. It is highly likely that not all satellites with identical coordination are active, and in fact the lack of data of decommissioned satellites by IARU is being acknowledged as a problem [29]. One benefit of the use of amateur frequencies is the possibility of radio amateurs globally assisting in the downlinking of data from the satellite. [28]

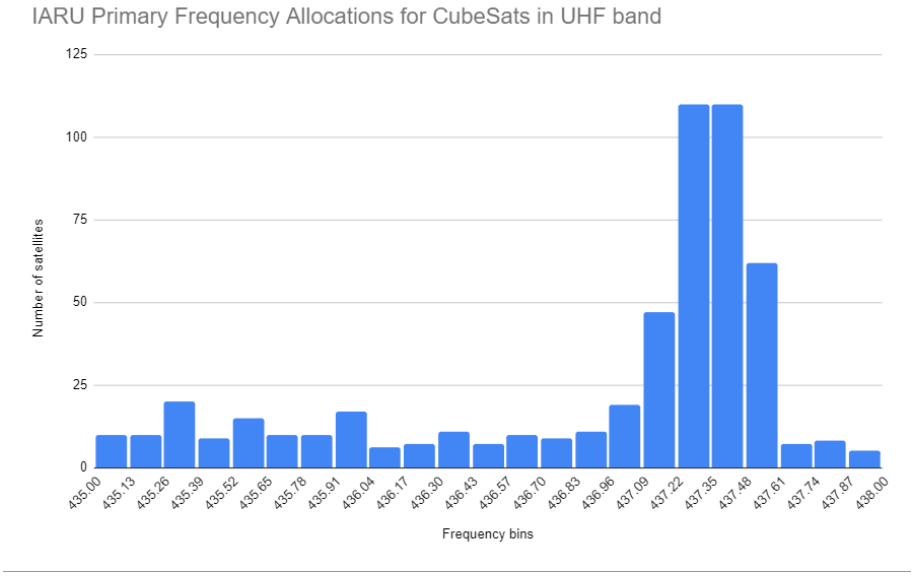

Figure 2: Histogram of IARU coordinated satellite project frequency allocations in the UHF band. Data scraped from [28]

2.2 Nanosatellite communication systems

A nanosatellite communication system (COM) is used to establish a link between the satellite and a ground station for the transfer of data and commands. The communications system is a part of the satellite bus, which typically also includes the electric power system (EPS), on-board computer (OBC) and the attitude control and determination system (ADCS). The bus is typically interconnected with a stack connector. [50]

A communications system for a nanosatellite typically consists of a microcontroller, transceiver circuit and additional signal conditioning components such as power amplifier, filters and a low noise amplifier.

The microcontroller is the brain of the communications subsystem. It communicates with the OBC and the rest of the satellite bus through some communication interface, typically a stack connector. The microcontroller has the program code running in the communications platform. The microcontroller controls the transceiver. The transceiver is an integrated circuit (IC) that does the frequency synthesis, signal modulation, demodulation, encoding and decoding as well as signal filtering and amplification [6]. When the transceiver IC receives messages, it communicates them to the microcontroller, which then typically communicates them to the satellite OBC. The top level diagram of a typical communications subsystem is depicted in Figure 3.

The block diagram is for a half-duplex communications system where the same transceiver handles both the transmission and receiving, but does not do both simultaneously. Additional filter and matching stages between the depicted radio frequency blocks are in practice required to ensure efficiency of the transmission and sensitivity of the receiver.

The purpose of the external low noise amplifier (LNA) is to reduce the noise figure

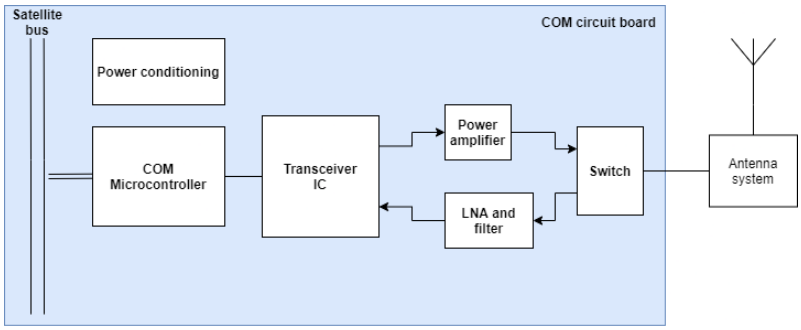

Figure 3: Typical communication system top level diagram for a CubeSat operating in the UHF frequency. The physical printed circuit board of the COM module is on blue background. The antenna system includes the antenna connectors and possible antenna power distribution and phasing network. Additional filtering of transmission and receiver path is also typically implemented at different points before the antenna.

of the receiver chain and in that way achieve better receive sensitivity. The power amplifier increases the, typically very modest, transmission power of the transceiver to a level of about 1 W of total transmission power. The radio frequency switch is required to separate the transmission radio signal path from the receive signal path. This is specifically true in a radio utilising half-duplex communications.

Many commercial off-the-self (COTS) transceiver integrated circuits available nowadays are fully configurable at UHF and VHF frequencies up to 1 GHz, such as the TI CC1125 [6]. The internal circuitry within the small form factor chip includes the all the functional circuitry required for the generation of the encoded modulated radio frequency signal as well as filtering, decoding and demodulating incoming transmission. The CC1125 transceiver circuit block diagram is shown in Figure 4 and represents a typical configuration inside a commercial integrated transceiver IC.

Some nanosatellites divide the radio frequency (RF) communication into two bands, one for uplink and one for downlink, allowing a full-duplex communication system. [4]. For example using the amateur frequencies in VHF for uplink and UHF for downlink. An alternative to the full-duplex system is to use the presented half duplexing in a time-division-duplexing (TDD) scheme, where the same band is used for uplink and downlink. In this scheme there is an agreement of the time windows, or slots, the uplink and downlink get during communication [58]. The complexity of a full-duplex system is higher because of the two frequencies, but such a system also might be necessary in cases where the uplink and downlink frequencies are allocated for one-way traffic only. This is actually the case in many of the bands allocated to satellites.

2.2.1 CubeSat transmit power

A nanosatellite communications system transmit power can be limited by the frequency coordination agreement, regulatory agreements on emission levels or typically more practical matters like the available satellite power budget or the power amplifier component selection.

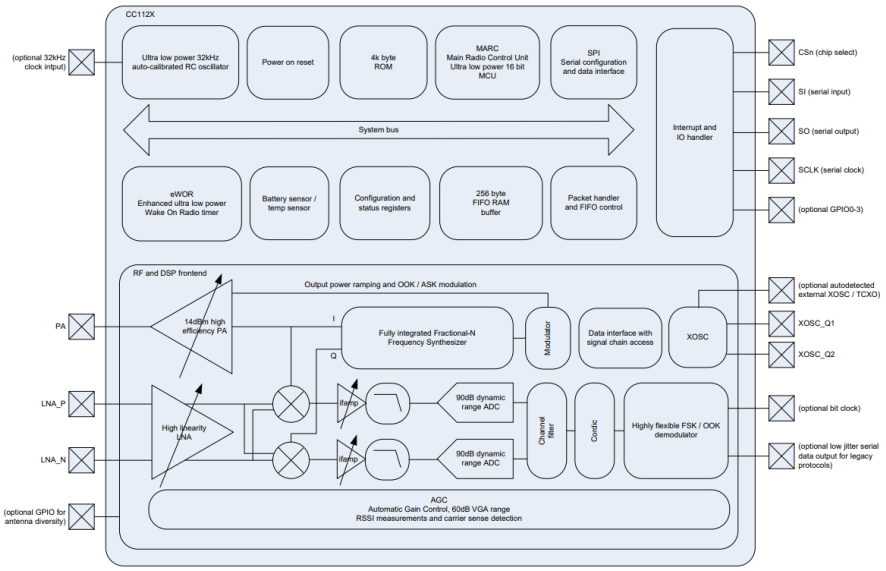

Figure 4: Transceiver internal block diagram. Most of a typical CubeSat radio frequency components of the transmit and receive path are inside the transceiver IC. Mainly the frequency synthesizing, modulation and demodulation, encoding and decoding, and the analog digital conversion.

Typically, the nanosatellte transmit powers were 1 W when using frequencies below 1 GHz, and below 1 W when using higher frequencies according to ITU, in a publication from 2014 [33]. The antenna gain for the VHF and UHF bands are low and the radiation pattern isotropic, whereas higher frequencies have a higher antenna gain. [33].

The antennas used in nanosatellites are often wire monopole or dipole antennas in the VHF and UHF frequencies and patch antennas in higher frequencies. The wire antenna needs to extend itself away from the frame of the satellite, which requires a more complicated structure, as the antenna has to be actively deployed after the satellite itself is deployed. The antenna radiation pattern is often made as isotropic as possible for nanosatellites. This is because the satellite and antenna orientation does not then have to be controlled. [33] At higher frequencies the available types of antennas get more directional. For S-band and higher, the patch antenna type is common, but a plethora of different antenna types have been created including helical, reflector, slot, horn and metasurface antennas. [1]

The transmit power together with the antenna generate the transmission of energy that will be available to the receiver. Therefore, smaller transmit power can be compensated with a more directional antenna through higher gain.

2.3 Commercial CubeSat communication systems overview

A small review of commercial communications subsystems in Table 1 shows typical values of power consumption, transmitting power and data rates for systems in the UHF frequency. It can be noticed that the four commercial systems are clearly

different in their marketed values.

Digging into the datasheet or operating manual can however reveal the real story behind the values that are first displayed. For example, the EnduroSat transceiver system gives the transmit power consumption in a state where the transmitter is on 50 % of the time [67]. The other systems show a value of actual maximum power draw [9], [31].

As the sensitivity depends on the baud rate as well as what is set as the error rate limit when determining sensitivity, the value given in the table can also be misleading. For example, the sensitivity could be given for a 1200 baud rate with a 1 % bit erro rate (BER). The bit error rate can then in reality be too high at this sensitivity power level for practical communication. This is something to keep in mind when drafting the first link budgets.

Table 1: Comparison of commercial CubeSat subsystem parameters. The data taken from manufacturer website or brochure. Transmit power range from 500 mW to 3 W and data rate maximum is between 9600 and 38400 bps. Sensitivity data is given often without definition of baud rate or BER value. [9], [31],[12],[48]

	EnduroSat	**NanoAvionics**	**AAC Clyde Space**	**ISIS Space**
Subsystem name	UHF Transceiver II	SatCOM UHF	PULSAR-TMTC	VHF/UHF FDT
TX Power (W)	1-2	3	2	0.5
Frequency band	UHF	UHF	VHF and UHF	VHF and UHF
Power draw TX (W)	1.4	-	5.5	4
Data rate (bps)	19.2	38.4	9600	9600
Sensitivity (dBm)	-121	-122 (2400 baud)	-115	-104 (BER 1e-5)
Price (Eur)	3500	-	-	8500

The power consumption of the transceivers varies between 1.4 W to 5.5 W, and show an efficiency between about 13 % and 70 % in transmitting mode, from worst to best. Again, for power budget reason it is necessary to look at how the manufacturer has measured the power consumption to ensure that things like duty cycle are considered correctly.

The advantage of using a commercial subsystem is in the time saved in designing and testing the subsystem itself. It can also be assumed that a commercial system is more reliable than a completely new design because of the ability for commercial manufacturers to comply with manufacturing quality standards and have more extensive test campaigns for their products. Additionally, the commercial systems have flight heritage, and thus have a higher technology readiness level. From the EnduroSat datasheet can be found the information that the EnduroSat UHF transceiver is tested against ECSS standard ECSS-E-ST-10-03C and NASA's GEVS standard GSFC-STD-7000A [12].

The use of a commercial subsystem however does not necessarily guarantee that the transmission spectrum of the overall system will be in compliance with the ITU recommendations. Therefore even a commercial subsystem should go through some tests to confirm compliance for example after integration to the satellite bus.

An example of a commercial subsystem is shown in Figure 5. This is an AAC Clyde Space commercial transceiver, which shows it uses the CubeSat PC/104 stack connector and has two SMA antenna connectors for the VHF and UHF antennas. The radio components are shielded in a screwed-on casing.

Figure 5: AAC Clyde Space commercial transceiver in PC/104 form factor. Image source AAC Clyde Space : https://www.aac-clyde.space/wp-content/uploads/2021/10/PULSAR-VUTRX-UTRX-also.jpg (Accessed 18.11.2021)

The commercial system review gives some reference values, or a bench mark, for important parameters when concidering designing a new custom subsystem for a CubeSat project or. Mainly the transmit power, subsystem power consumption and the sensitivity performance.

2.4 CubeSat communications system failures

A survey of 178 CubeSats conducted in 2014 showed that CubeSat reliability was much lower than the reliability of other spacecrafts. A common outcome for CubeSats was "death on arrival" (DOA). The DOA status means the satellite is launched and deployed but no contact was ever made from the ground station to the satellite. The second most critical failure period was the first 100 days in orbit. The overall failure rate was estimated to be about 50 %. Subsystem specific failure analysis showed that the COM subsystem is responsible for almost 30 % of failures. [43]

The reason behind the high number of failures was suspected to be mainly the fast pace and budget concerns of typical CubeSat projects. The authors of the article suggest that more functional testing, instead of more qualification tests, of the complete satellite system could potentially solve the majority of the problem. [43]

A very similar statistics for "small satellites" category are presented by a paper on the statistics on failure rates, where the rate is 41.3 % between the years 2009 and 2016, including the launcher failures. [40] Also, the use of COTS components and their reliability is suggested as potential failure reason, as well as lack of testing, reduncancy and shielding. Also, the errors in workmanship play a role in reliability. The small form factor of a CubeSat puts constraints on the system design and implementation and generates unwanted single points of failures. [43], [15]

In order to determine the cause of death of a CubeSat, telemetry is required. EPS telemetry can tell a lot about how a satellite is operating and which subsystem is potentially failing. For example, MicroMAS satellite telemetry gave information that led the team to determine the probable cause of death was the communications subsystem. This was seen from the power consumption data that showed the communications subsystem was not pulling power required for normal transmission. The team also deduced that the communications subsystem power amplifier, which had been repaired just prior to satellite delivery, had failed. [14]

A lot of the risk mitigation for a CubeSat is in proper testing. Testing at subsystem or component level is important, but do not guarantee the satellite operates once all subsystems and payloads are integrated. For a communications subsystem the power supply and noise conditions within an integrated satellite obviously differ from a subsystem level test bench condition. This is why integrated satellite testing is always necessary.

2.5 Regulations and standards for CubeSat communications

The microwave spectrum is recognized as a limited resource, and therefore the use of it is limited by allocations and regulations through international agreements. As the nanosatellite industry grows, to include more small experimental satellites, educational satellites and commercial ones, so does the need for microwave spectrum use. The trend of need for short period licenses for satellite communication is recognized by the International Telecommunications Union. In the World Radiocommunication Conference 2019 (WRC-19), ITU started processes to make the regulatory procedures easier for satellite projects requiring a license lasting a maximum of three years, consisting of a maximum of ten satellites. [51], [68]

As a result of the WRC-19 conference, and to ensure interference free microwave spectrum use, ITU is developing a small satellite handbook. The handbook offers education on the regulations, registration and coordination process as well as technical information concerning small satellites. [68]

Frequency coordination or registration is an essential part of a CubeSat project. The process is required for the legal use of a certain band in the microwave spectrum. However, in order to use the band as intended, additional attention is required to the limitations to transmission spectrum, as emissions outside the coordinated band are not allowed. The best way to ensure an interference free radio communication is to follow some radio frequency standards and ITU recommendations.

2.5.1 Frequency coordination

The use of radio frequency spectrum is regulated at a global scale with international agreements. The top governing agency for the whole spectrum is the International Telecommunications Union. Different frequency bands are allocated for different use cases based on the industry, geography or users such as radio amateurs. [39]

The registration and coordination of any frequency for nanosatellite use always happens through ITU. If amateur radio frequencies are used, then International Amateur Radio Union coordination is additionally required [29]. Typically, the frequency coordination with ITU is handled through a government regulatory agency responsible for radio frequency use within the country. In Finland the governing agency is TRAFICOM [65]. Some frequency bands are not subject to coordination, but a registration process is still required through ITU where notification of the band to be used as well as space object registration will be required. Additional requirements for the license may also be set by the national regulatory agency. [68]

The accepted coordination of a frequency for a satellite with ITU and IARU results in an agreement on the frequencies allowed for downlink and uplink together with an EIRP maximum value and emission designators. The emission designators include information on the necessary bandwidth, modulation type and modulation nature as well as the information type included in the signal. [8]. The IARU coordination agreement also specifies an earth command station, planned orbit of the satellite, licensing administration and the launch date. [69]

The use of amateur-satellite service spectrum is only for missions that meet the requirement for an amateur-radio mission. The exact requirement is defined in ITU Article 1 as follows "A radiocommunication service for the purpose of self-training, intercommunication and technical investigations carried out by amateurs, that is, duly authorized persons interested in radio technique solely with a personal aim and without pecuniary interest." [32] If the amateur-satellite requirement is not met, then other frequencies allocated for space use must be coordinated outside of IARU.

The main purpose of regulating the radio spectrum use is to enable its usage efficiently and rationally by minimizing potential interference to radio communication from man-made sources. In practice this means limiting the frequency use so that a device only uses the necessary bandwidth required and does so in the coordinated frequency band. The emission outside the allowed band is divided into two domains, the out-of-band domain and the spurious domain. The out-of-band domain covers the emission spectrum close to the allowed emission band, to a separation of 2.5 times the necessary bandwidth. The spurious domain is the spectrum outside the necessary bandwidth and out-of-band domains. The ITU recommendations contain emission limits for a satellite for both of these domains. The ITU-R SM.1541 recommendation provides the out-of-band emission limits, and the spurious domain limits are given in ITU-R SM.329. [35]

2.5.2 Standards applicable for CubeSat radio testing

Many CubeSat projects are built in a fast pace with low budgets. This also affects the testing methodology and focus. The main focus may be to perform testing necessary

to meet the launch requirements and confirm basic operations. The application of an industry level development and verification process would be unnecessarily complex for a CubeSat project.

In order to better meet the needs of a CubeSat project, The European Space Agency (ESA) has produced a document "Tailored ECSS Engineering Standards for In-Orbit Demonstration CubeSat Projects". The document covers the ECSS standards, and their subsections, that are to be used in certain ESA CubeSat projects. [16]

Selecting standards appropriate for the testing of a communications subsystem from the abovementioned tailored list of standards, is shown in Table 2. This table includes those standards from the tailored list of ECSS standards generated by ESA that the author of this thesis sees suitable for the testing of a radio subsystem. Any mechanical and material specific standards albeit being applicable also to the communications subsystems are omitted from this table. The resulting table has four standards. Two of them focus on the communications subsystem, and two are more general standards.

Table 2: Applicable ECSS standards for testing a CubeSat communications subsystem. This list is an abbreviated list from ESA tailored list of ECSS standards [16]

ECSS number	**Title**	**Issue**
ECSS-E-ST-10-03C	Testing	1 June 2012
ECSS-E-ST-20C	Electrical and electronic	31 July 2008
ECSS-E-ST-50C	Communications	31 July 2008
ECSS-E-ST-50-05C Rev.2	Radio frequency and modulation	4 October 2011

The first standard in the list with the title "Testing" includes a vast amount of testing procedural requirements such as test plan documentation, test conditions and many mechanical and environmental tests. The standard is however describing the testing at a general level, and does not consider specifically the communications system parameters. For this reason it is not the most useful tool for testing the communications subsystem. [17]

The second standard of the list "Electrical and electronic" has many parts applicable to the communications subsystem, and things to be considered in the component selection phase such as the component power handling capability and isolation between the receive and transmit side. Additionally, this standard puts some focus on the antenna interface and performance. The scope of this thesis does not extend to the antenna system, but to keep the test bench complete, these tests are necessary. [18]

The "Communications" standard is the most applicable of the standards for the communications subsystem developer. It describes the process of developing a system from scratch. The standard divides the process into three stages: Analysis stage, design stage and implementation stage. Before starting with the analysis stage, the system requirements and specific subsystem requirements are to be generated. The

analysis stage process includes feasibility analysis, technical analysis of link margins and data rates, definition of architecture, definition of verification and testing plan, identification of solutions for realization of the COM system and other higher-level activities. The main outputs at this stage are the link margin analysis, criticality analysis report and system verification plan. [20]

The next stage in the standard is the design and configuration stage, where the potential implementation of the subsystem is divided into individually realizable components. The components are named and given their own requirement specifications. At this stage the link margin analysis is updated.

The final stage is the implementation, where the components are realized, integrated and tested. After the implementation the link margin analysis is yet again updated. [20]

The communications standard also gives some higher-level requirements for the subsystem, such as commandability and telemetry capability at all attitudes and rates. More parameters mentioned in this standard are included in Figure 3.

The "Radio frequency and modulation" standard focuses on the emission spectrum and modulation types. The standard gives some parameters for power flux density limits at specific frequencies to protect certain terrestrial radio astronomy bands as well as occupied bandwidth limits for S-band and higher frequencies.[19] The parameters that can be concidered applicable to a CubeSat project are mentioned in Figure 3.

Another standards organization that has an applicable standard publication for radio device testing is the European Telecommunications Standards Institute. The ETSI EN 300-220-1 V3.1.1 (2017-02) standard "Short Range Devices (SRD) operating in the frequency range 25 MHz to 1 000 MHz; Part 1: Technical characteristics and methods of measurement" includes not only many parameters to test for, but describes in enough detail the proper procedure to perform the tests. [21]

The comparison of parameters mentioned in the ETSI standard and the ECSS standards can be seen in Figure 3. The overlapping tests include testing for the transmitter power, receiver sensitivity, frequency stability, emission spectrum and bi-directional operation. The contents of this table is further assessed in Chapter 4 of this thesis when a test bench for the communications subsystem is considered.

2.5.3 Emission limits

The emission limits for a radio device operating at the amateur UHF band are given both by ETSI and ITU in their standards as emission masks or numeric formula. The emission limit for the out-of-band domain in the ETSI standard is given as a mask in Figure 6. The same domain mask from the ITU is given in Figure 7. There are some differences in the mask limits. Specially as the ETSI standard requires the out-of-band emissions as absolute, in certain regions, whereas the ITU recommendation power limit is relative to the emission power. Ultimately the mask provided by ITU is more generally binding as it is specifically given for space stations operating in the amateur frequencies. The applicable mask depends on the frequency band at which the device operates, and different masks and limits depends on emission power and

Table 3: Parameters and tests from three ECSS standards and ETSI-EN 300-220-1 standard. The overlapping parameters between ETSI and ECSS are clearly important to consider in any radio system. Some ETSI receiver side tests from this standard could be unnecessary.

Parameter	**Electrical and electronic**	**Communications**	**Radiofrequency and modulation**	**ETSI EN 300 220-1 V3.1.1**
Link budget	X		X	
Signal to noise ratio	X			
Transmitter power	X			X
Receiver sensitivity	X			X
Intermodulation products	X			
Multipaction	X			
Corona	X			
Spectral purity	X			
VSWR	X			
Frequency stability	X		X	X
Antenna performance	X		X	X
Insulation between transmitter and receiver	X			
EIRP	X			X
Component power handling	X			
RF power emission limits		X		
Link protocol		X		
Doppler shift		X		
Tumbling		X		
Failure modes		X		
BER rate and frame rejection		X		
Data rates		X		
Frequency selection		X	X	
Unwanted RF emissions		X	X	X
Cessation of emissions		X	X	
Modulation selection			X	
Subcarriers			X	
Carrier phase noise			X	
Ground network compatibility			X	X
Duty cycle				X
Transient power				X
Operation in low voltage conditions				X
Adaptive power control				X
Adjacent channel selectivity				X
Spurious response rejection				X
Blocking				X
Polite spectrum access				X

frequency band. [36] [21]

Outside the out-of-band domain the spurious domain limits apply. From ITU recommendation ITU-R SM.329-12 the spurious domain emission limits for a space service space station is given as $43 + 10 \log P$, or 60 dBc, whichever is less stringent, in a 4 kHz reference bandwidth [37] [35]. The ETSI standard gives a mask for the spurious domain, and it is shown in Figure 8. The comparison of the two is more difficult this time, because the reference bandwidth is different. The ETSI standard additionally has separate domains again depending on how far we are from the operating channel. Assuming the transmit power is 0 dBW, the ITU limit for the whole spurious domain is −43 dBc [35]. Since the 4 kHz bandwidth is four times larger than the 1 kHz bandwidth, this results in a 6 dB difference. That means the emission limit of −36 dBm / 1 kHz is the same as −42 dBm / 4 kHz making the ITU standard more stringent in the domain closest to the operating channel. However, in the next domain, at 4 times the operating channel width (OCW) distance, the ETSI emission mask lowers by a decade. The same happens at the next domain change at 10 times the OCW. The rest of the spurious domain therefore requires an emission limit of −62 dBm, or −62 dBc for a 1 W transmitter, being much stricter than the ITU standard.

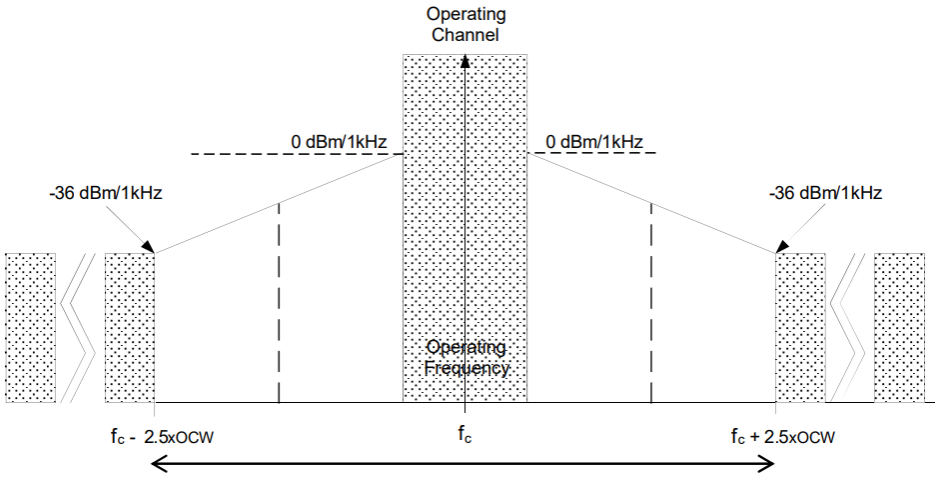

Figure 6: OOB emission limit mask from the ETSI 300 220-1 standard. [21]

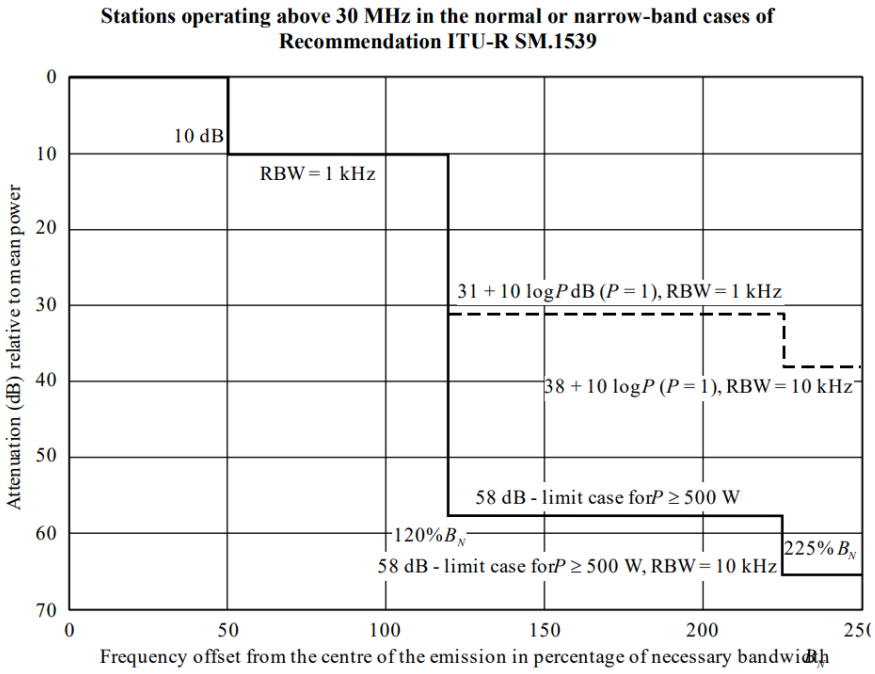

Figure 7: OOB emission limit mask from the ITU-R SM.1541-6. [37]

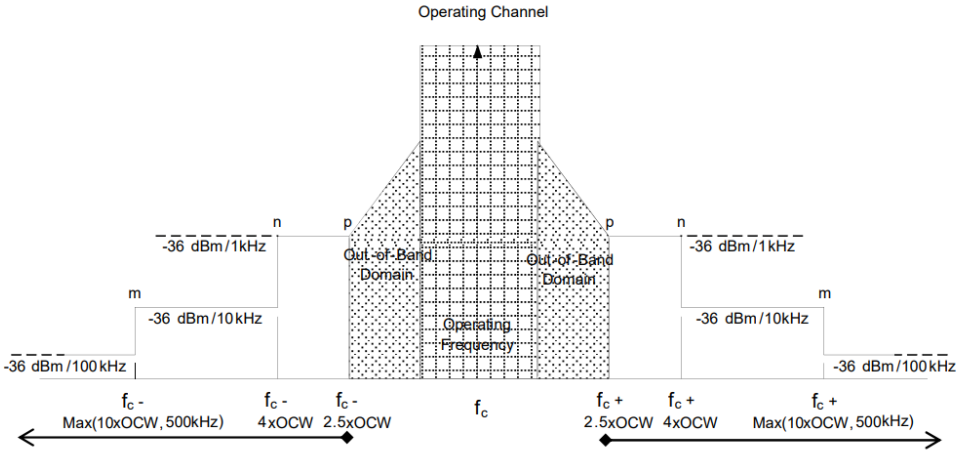

Figure 8: Spurious emission limit mask from the ETSI 300 220-1 standard. [21]

2.6 Review of CubeSat radio testing

From available published documents of tests performed for nanosatellite communications systems, a review is gathered in Table 4. The table shows an 'X' for a test or analysis that was performed or mentioned in the document. The table should not be read to show that some tests had not been performed, as many tests are probably performed but not in the publication.

The link budget was shown or mentioned in many of the publications. The link budget was laid out for the uplink and downlink and in the case of the BIRDS-I satellite, for four different types of downlink modulation [57]

Simulation tools were presented in some of the publications. Three publications showed the use of an EM simulation tool for the simulation of either the antenna or RF filter stages, when the filter stage was made of microstrip. Only one paper clearly showed the use of a simpler linear circuit simulation tool in the design process.

The doppler effect was considered also by either varying the transmit frequency of the ground station in a long-range test or by generating the doppler shift in lab conditions with a circuit generated doppler shift.

The long-range communications test was shown in three papers. With the ability to add attenuation into the communication line, some understanding of sensitivity of the satellite receiver was gained. The sensitivity measurement done this way is marked in the table with a 'V' in the sensitivity column.

Component level analysis was a common theme, with attention being put into the comparing and selecting components for a communications system. Typically, this consisted of some type of trade study. Components such as the transceiver, PA and LNA were of typical concern.

It should be noted that the publication on PolySat was the only thesis on this list, and the focus of this thesis was the development of a new S-band radio for PolySat. The other publications were published papers. This explains the difference in the number of tests included in this document.

Some other theses that explained the testing procedure for a CubeSat communications system included theses by other students of the Cal Poly CubeSat development program. The program has developed and launched multiple satellites during over two decades of operation [5]. The maturity of their program has allowed for very specific and detailed studies of the system during the development of their radio systems. One thesis focusing purely on the UHF radio sensitivity testing found that the Cal Poly team required a Faraday cage for the suppression of outside interference and radio leakage from transmitter used in the test. The thesis also shows tests benches performing LNA matching and measurements of LNA gain as well as the noise figure. Because of a noise issue in their original design, multiple configurations of power supply were tested to see if power supply noise from switching regulators would cause more noise than linear regulators. This is done through essentially iterative process, and the findings show no difference between switching regulators and linear regulators. [5]

Another thesis from the PolySat team describes the design for a UHF communications system, which was done to improve older designs. The tests and steps

taken to develop the system described in this thesis consists of setting system requirements, a component level trade study, careful layout of radio frequency components, impedance matching through VNA measurements and Smith chart through iterative process, noise figure measurement, power amplifier efficiency testing at different operating voltages and input powers, measuring and mitigating spurious harmonics, sensitivity measurement of the receiver at different baud rates and modulations, tuning the center frequency and finally long range testing. [71] This was one of the most extensive test campaigns, and included one of the very few pubications that took any interest in emission spectrum outside the occupied band.

Aalto University has also heritage from previous CubeSat projects, and a thesis designing an S-band transmitter describes the process of creating a custom S-band device for a CubeSat. The testing involves impedance matching using simulations and measurements, power amplifier measurements and ideas for a load-pull method of PA matching as well as failure mode analysis. [60]

An example of a test bench when using a commercial system presented in a paper describing the EIRSAT-1 CubeSat functional verification tests. The satellite project is supported by ESA's Fly Your Satellite! program. The verification test involving the communications subsystem tests whether or not the COM successfully performs the following 5 tasks: Reset OBC when receiving DTMF tone, use VHF to uplink packets, use UHF to downlink packets, transmit beacon every 90 seconds, cease and restart beacon and radio transmissions. [70]

Table 4: Table of different test parameters performed concerning the communications subsystem in different satellite projects. The tests performed depend on publication focus. X marks testing of parameter is performed, V marks for the receiver sensitivity mark some sensitivity information was measured as a part of long range testing.

Parameter	**OPTOS**	**PilsenCUBE**	**S-band proposal**	**ISM S-BAND RADIO FOR POLYSAT**	**SIGMA**	**BIRDS-I**	**COTS-based RF Receiver**	**DVB-S2 Experiment**
Link budget			X	X	X	X		
Ground segment analysis	X	X		X	X			
Component level analysis	X	X	X	X			X	
Radiation consideration	X	X						
Antenna measurements			X	X	X	X		
Simulation, Linear			X					
Simulation, EM			X			X	X	
Frequency licensing				X				
Receiver sensitivity				X	V	V		X
Doppler				X	X			X
PA protection circuitry				X				
Visual inspection				X				
Use of RF test points				X				
TX power				X				
TX Power range				X				
RX sensitivity testing				X				
Long range communications test					X	X		X
Short range communications test					X			
Component level testing				X			X	
Modulation testing								X

2.7 Radio frequency communication theory

For a successful link between the ground station and the satellite to be established, there are several factors that have to be taken into account. The process of examining the properties of the link is the link analysis. The result of performing link analysis is the link budget, which tells whether the communication is plausible with the selected system and operating conditions. The link capability is described by the error probability, and it can be estimated for a given modulation scheme from the signal to noise ratio (SNR) or E_b/N_0. The limit for an acceptable error probability should be decided beforehand. The link budget is a table of values including all the noise sources, gains, losses and power involved in the radio frequency communication process. From the link budget a link margin is calculated. The link margin tells how much confidence there can be that the system performs to expectation. [59]

The signal to noise ratio for a digital signal can be written as [59]

$$\frac{S}{N} = \frac{E_b}{N_0} \cdot \frac{f_b}{B}, \tag{1}$$

where E_b is the energy per bit, N_0 is the B is channel bandwidth and f_b is the channel data rate. The value E_b/N_0 is the signal to noise ratio normalized by the bandwidth and bit rate. The E_b/N_0 value is a dimensionless value and is used to measure a communication system performance. A low requirement for E_b/N_0 from a receiver means it performs with a lower error rate at the same signal strength. [59]

The link budget is calculated for the worst-case SNR for the channel, and is used to determine if a link is possible and reliable. Typically, a link margin of 6 dB is a requirement for a satellite link budget. [4] However if the system and conditions are well known and taken into account in the link budget, a link margin as low as 1 dB could be designed [59]. As the transmission power and losses for both uplink and downlink are typically different, two link budgets are drafted.

2.7.1 Free space path loss

Largest contributor for attenuation in a satellite link is the free space path loss (FSPL). It is the attenuation of energy between the two antennas resulting from the spreading of the transmitted signal power into space. It depends on the distance between the two antennas and is included in the Friis power transmission equation which gives the overall power ratio between the received and the transmitter.

The Friis transmission power equation is [53]

$$\frac{P_r}{P_t} = G_t G_r (\frac{\lambda}{4\pi R})^2, \tag{2}$$

where P_r is the power received, P_t is the power transmitted, G_r is the gain of the transmitting antenna, G_t is the gain of the receiving antenna, λ is the wavelength and R is the distance between antennas. The Friis formula gives the ratio of the transmitted power to the received power. The received power can be easily calculated from this equation.

The gains of the transmitting and receiving antennas are measurable quantities, or they can for example be taken from manufacturer datasheet. The remaining term is the FSPL, or attenuation from the signal propagating through space. The free space path loss L_s is given as [59]

$$L_s = (\frac{4\pi R}{\lambda})^2, \tag{3}$$

Or equivalently in decibels, expressing R in kilometers, f in megahertz [58]

$$L_{s(dB)} = 32.4 + 20 \log R_{km} + 20 \log f_{MHz} \tag{4}$$

The free space path loss for satellite communication works well as the only attenuation factor in UHF frequencies because the medium between the satellite and ground station is mostly empty.

2.7.2 Modulation schemes

Modulation means how the signal is changed over time in order to convey information. The main modulation schemes used in CubeSats are amplitude shift keying (ASK) for the use of a beacon that transfers basic satellite health telemetry, and frequency shift keying (FSK) or phase shift keying (PSK) for main data transmission. [11],[42]

In frequency shit keying, the data is conveyed by changing the frequency over time. For binary FSK (BFSK) one frequency represents a bit value 1 and another bit value 0. BFSK is a special case of FSK, as more than two frequencies can be used to represent more than one symbol at a time. The frequencies in FSK implementation are usually chosen to be orthogonal. The orthogonality of the FSK frequencies means the tones are uncorrelated over the time each symbol is transmitted. The requirement for two tones to be orthogonal is that the frequency separation is 1/T, where T is the symbol time. This is because the minimum frequency separation for two orthogonal tones of BFSK can be analytically shown to be $\frac{1}{2T}$. Using minimum frequency separation requires less bandwidth to be used for the same data rate. [59]

The use of bandwidth is typically very limited in the UHF and VHF bands, and minimizing the bandwidth use is encouraged. The occupied band width (OBW), or transmission bandwidth B_T can be estimated with Carson's Rule: [10]

$$B_T = 2\Delta F + 2B, \tag{5}$$

where ΔF is the frequency deviation and B is the bandwidth of the modulating signal. The frequency deviation is the frequency difference of the carrier and the frequency representing bit value 0 or 1. The deviation is half of the frequency separation.

For example we can try calculating the occupied bandwidth for an FSK square wave modulated signal with a baud rate of 9600 and a deviation of 2400 kHz. We can calculate the occupied bandwidth as follows. The bandwidth of a 9600 baud rate signal is $B = \frac{9600}{2}\text{Hz} = 4800\,\text{Hz}$. This can be understood by thinking of an alternating '010101' transmission, which has the highest modulation frequency. In this waveform, a bit time interval is the time the square wave spends at the value

'0' or '1', but the modulating frequency is a full waveform including a '01' or '10. Therefore, the highest modulating bandwidth is half the baud rate for BFSK. Then according to Carson's rule, the occupied bandwidth of the FSK signal modulated by this square wave is given as

$$\mathrm{OBW}_{Carson} = 2 \cdot 2400\,\mathrm{kHz} + 2 \cdot 4800\,\mathrm{kHz} = 14.4\,\mathrm{kHz}. \tag{6}$$

When the FSK modulated signal is switching between two frequencies, the attempt to immediately change from one frequency to another results in emissions in frequencies higher than modulating frequency, potentially outside the allowed band. For this reason, switching from one frequency to another is done through a gaussian filter, so that the transition between the two frequencies is essentially done through a low pass filter. [10] When in addition to using minimum shift keying, a gaussian premodulation filtering is used, the occupied bandwidth of the transmission can be reduced even further. The resulting modulation scheme is called Gaussian minimum shift keying (GMSK). [66]

Another formula for calculating the occupied bandwidth, or necessary bandwidth B_n, is given in ITU recommendation SM.853-1 , where the necessary bandwidth is defined as containing 99 % of the power. This is given specifically for GMSK modulation as

$$B_n = \frac{R}{\log_2 S + 2DK}, \tag{7}$$

where R is the bit rate, S is the number of signalling states, D is the frequency deviation and K depends on filtering. It is given as $K = -0.28$ for the necessary bandwidth containing 99 % of the power. [38]

The ITU formula gives a necessary bandwidth for the same example as before to be

$$B_n = \frac{9600\,\mathrm{Hz}}{\log_2 2} + 2 \cdot 2400\,\mathrm{Hz} \cdot (-0.28)\mathrm{Hz} = 8256\,\mathrm{Hz}. \tag{8}$$

There is a significant difference in the two estimates, and it should be noted that the Carson's rule in this form overestimates the bandwidth required for a filtered digital modulated signal.

The frequency modulation index (β_f) is given as [10]

$$\beta_f = \frac{\Delta F}{B}, \tag{9}$$

which can be calculated for the same set of values in previous examples to be

$$\beta_f = \frac{2400}{4800} = 0.5. \tag{10}$$

This is in fact the frequency modulation index requirement for any MSK signal, as the tone spacing for MSK is always half of the bit rate, resulting in a deviation of quarter of the bit rate. [59]

It is possible to use also the phase information in some cases of the frequency shifted keying modulation scheme. This type of scheme is called coherent FSK, and

it requires the phase relationship of each tone to be fixed. This is typically done by setting the transmitted signal to have a separation of integral multiple of baud rate. Non-coherent FSK is simpler to generate as the phase can be variating randomly. The difference of the two is the cost is about 1 dB more E_b/N_0 required for the same BER. [56]

The calculated theoretical minimum bit error rate for different E_b/N_0 and different modulations is shown in Figure 9. It is clear that using non-coherent FSK has a poor E_b/N_0 performance compared to PSK for binary case. The ability to use coherent MSK offers nearly the same performance as PSK in terms of E_b/N_0.

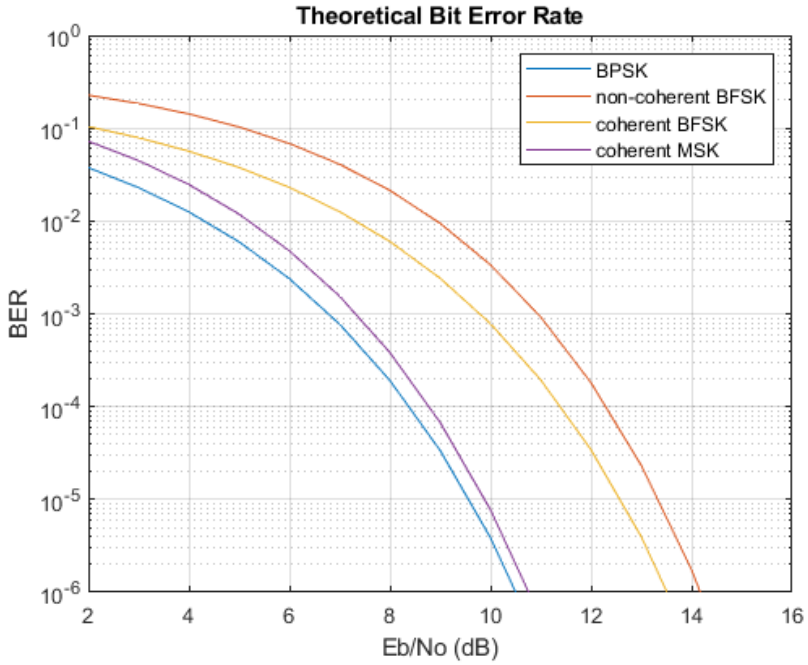

Figure 9: Bit error rates for different modulation types in an average white gaussian noise channel. For a BER of 10^{-4} the E_b/N_0 values for the non-coherent BFSK is about 12.5 dB and for coherent MSK 9 dB. The results are given by Matlab's signal processing toolkit's "berawgn" function.

The difference between the E_b/N_0 requirements for different modulations is significant. For signals requiring high sensitivity, when working with small transmit powers at great distances, the phase shift keying shows the best performance. It would be a natural choice for a modulation from the ones simulated. However, when using multiple bits per symbol, such as in QPSK, more E_b/N_0 is actually required when compared to QFSK. This is because FSK modulation will spread the information over a wider bandwidth, utilizing different frequencies, whereas PSK will keep the same bandwidth. This is why FSK is better for power limited systems, and PSK for bandwidth limited systems. [59]

2.8 Microwave transmission lines and impedance matching

The transmission of microwave power efficiently requires the electromagnetic waves to be guided. In a circuit board this can be done with microstrip transmission lines. A microstrip consists of a metal strip and a metal ground plane, separated by a dielectric substrate. For a wave traveling in one direction in the transmission line, the ratio of voltage and current at any point in the transmission line is called the characteristic impedance. The characteristic impedance Z_0 of the transmission line is given by

$$Z_0 = \frac{d}{w}\eta, \tag{11}$$

where d is the thickness of the substrate, w is the width of the transmission line and η is the intrinsic impedance of the dielectric medium given by

$$\eta = \sqrt{\mu\epsilon}, \tag{12}$$

where μ is the permeability of the medium and ϵ is the absolute permittivity of the medium. [7]

For a microstrip, the electromagnetic field is partially contained within the printed circuit board substrate of a typical relative permittivity of 4, while some of the field passes through air or vacuum of a relative permittivity of 1. This results in an effective permittivity somewhere in between the two. Figure 10 depicts how the electric and magnetic field lines behave around a microstrip transmission line [53].

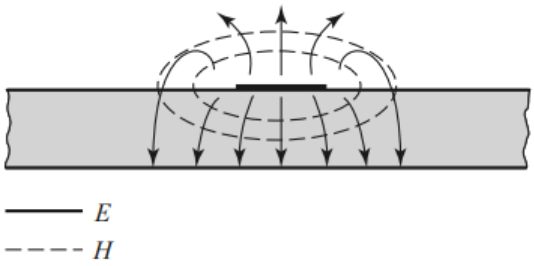

Figure 10: The electric and magnetic fields around a microstrip line. The fields are partially in the air and partially in the substrate. This causes the effective dielectric constant to be lower than that of the substrate only. [53]

When a transmission line with a characteristic impedance is terminated with an unequal load impedance Z_L, a reflection occurs. The reflection coefficient Γ describes the ratio of amplitudes of the incident and reflected voltages at the load. The reflection coefficient is given by [7]

$$\Gamma = \frac{Z_L - Z_0}{Z_L + Z_0}. \tag{13}$$

A non-zero reflection coefficient gives rise to a standing wave in the transmission line. Standing wave ratio (SWR) tells the ratio between the minimum and maximum

voltages, V_{min} and V_{max} along a terminated transmission line and is given by [7]

$$\text{SWR} = \frac{|V_{max}|}{|V_{min}|}. \tag{14}$$

The SWR is an easily measurable quantity and thus allows one to measure the mismatch of a load such as an antenna. The SWR and the reflection coefficient are related by the formula

$$\text{SWR} = \frac{1 + |\Gamma|}{1 - |\Gamma||}. \tag{15}$$

The transmitted portion of the electromagnetic wave at the impedance boundary is described by the transmission coefficient

$$T = 1 + \Gamma = \frac{2Z_1}{Z_1 + Z_0}. \tag{16}$$

Instead of the transmission coefficient, insertion loss, IL is used to describe the ratio of power passing through the circuit to the power put into the circuit. Insertion loss is defined as

$$\text{IL} = -20 \log |T| \text{ dB}. \tag{17}$$

The return loss, RL tells the ratio of power put into the circuit to the power returning to the source. Essentially this is a reflection coefficient, and is defined as

$$\text{RL} = -20 \log |\Gamma| \text{ dB}. \tag{18}$$

S-parameters are a useful tool to describe reflection and transmission within a circuit. A scattering parameter is defined as [53]

$$S_{ij} = \frac{V_i^-}{V_j^+}|_{V_k^+ = 0 \text{ for } k \neq j}, \tag{19}$$

where V_i^- is the reflected wave amplitude out of port i when port j is driven as V_j^+ when the rest of the ports (k) are terminated by matched loads. For a two-port network this means that S_{11} describes the reflection coefficient when port 2 is matched, and S_{21} describes the transmission coefficient when port 2 is matched. [53].

The S-parameters are the actual parameters measured by a vector network analyzer (VNA), which then calculates parameters such as SWR, return loss and impedance from this data. [53]

Impedance determination and transmission line calculations can be done with the help of a widely used graphical tool known as the Smith chart. The chart is a normalized resistance and reactance plot in a reflection-coefficient plane. The Smith chart is a typical part of many CAD software and test equipment for its visualization capability.[53] An empty Smith chart is shown in Figure 11

Essentially the center point of the Smith chart is the point that has the characteristic impedance, which is normalized to the value $1 + 0j$. Typically, this is $50\,\Omega$ for a transmission line. The load impedance is another point on the Smith chart, defined for a specific frequency. The distance between the load impedance point and

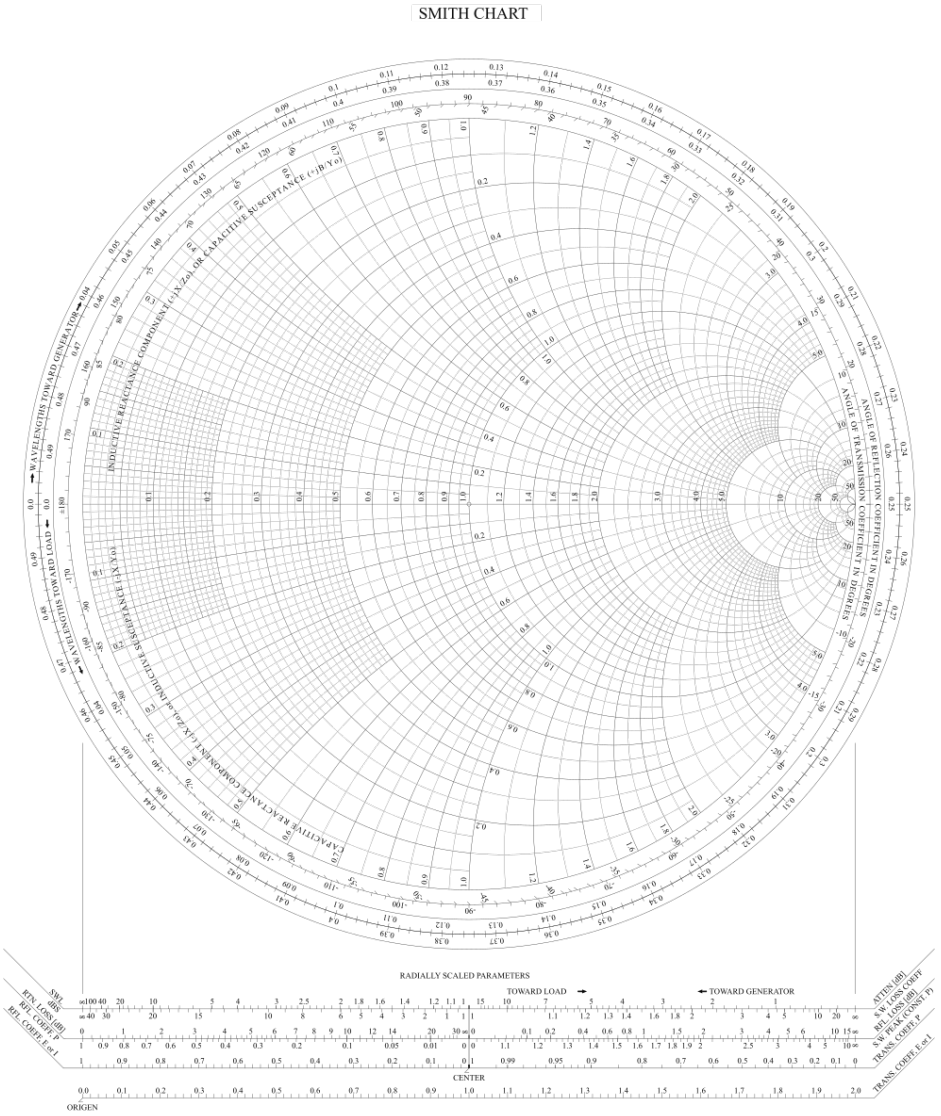

Figure 11: Empty Smith chart. The Smith chart is a graphical tool for transmission line calculations and impedance matching. The Smith chart is a typical output of a measurement device such as a VNA, or a CAD tool such as CST studio. Image source : https://upload.wikimedia.org/wikipedia/commons/7/74/Smith_chart3.svg fetched 18.11.2021

the center point on the graph tells the reflection coefficient. The further the load point is from the center point, the larger the magnitude for the reflection coefficient, and the poorer the matching. The key to matching a transmission line to a load is to move the load impedance to the center of the Smith chart. This can be done in practice by changing the lumped element values withing the device under test.

2.8.1 Radio frequency filters

Filters are used in the transmission and receiver side of the radio chain. The purpose of a filter is the selection of certain frequencies to pass while suppressing others. A filter is described by the insertion loss in the pass band, the pass band frequencies and the signal suppression outside the filter. The sharpness of the filters transition from pass band to the out-of-band is described by the quality factor, Q. A higher Q-value means the transition happens within a shorter band. [47]

Using lumped elements in filters is only applicable in lower radio frequencies. Even at lower radio frequencies specially made capacitors and inductors are required, as the parasitic losses and stray capacitances make typical components behave poorly. At higher frequencies even lumped elements become unusable, and methods utilizing waveguides and transmission line segments become the main ways to achieve filtering. Additionally micro electromechanical systems (MEMS) devices and surface acoustic wave filters can be applied at higher frequencies. [47]

2.8.2 Noise in a radio system

Noise is generated by thermal movement of components. The noise power from a matched load on a transmission line is given by [53]

$$P_n = kTB, \tag{20}$$

where k is the Boltzmann constant, T is the physical temperature of the load and B is the observed bandwidth.

The brightness temperature of a source depends on its physical temperature and equates to the amount of power it radiates. The received thermal noise of an antenna depends on the brightness temperature of the targets within the antenna beam. The overall power being the integrated power over the whole antenna beam. The sky has a brightness temperature of 2.7 K, whereas the ground has a brightness temperature of 300 K.[26]

When antenna is pointed at the sky, the brightness temperature and therefore the overall noise floor should be much smaller than for an antenna pointed from space to ground.

3 Foresail-1 communications subsystem analysis

The Foresail-1 COM system has two main functions. Primarily it acts as the data link between the Aalto ground station and the satellite on-board computer. Secondly, the Foresail-1 COM system will act as a message repeater for radio amateurs.

The system utilizes a half-duplex system using a time-division duplexing communication scheme. The radio is always active, which means the radio either transmits or receives at any given time. The operational capability of the radio is in the 70 cm amateur radio band.

The design of the Foresail-1 COM subsystem had already been done at earlier in the project, before the start of this thesis work. Initially the goal of this thesis was to create a test bench for the verification of the COM system radio performance. The initial testing however revealed that the system was not operating ideally. This extended the scope of this thesis to include design and implementation verification of the radio frequency circuitry.

One of the key design aspects for the Foresail missions is the reliability requirement. The component selection for the mission is based heavily on flight heritage, radiation tolerance and expected reliability while still using COTS components. In order to increase the reliability of the COTS components, automotive grade components are used whenever possible.

This chapter covers the analysis, design and implementation steps taken to improve the Foresail-1 UHF Communications subsystem radio frequency section. Foresail-1 has coordinated its radio license with IARU, ITU and TRAFICOM to a center frequency of 437.125 MHz. The coordinated effective isotropic radiated power is 1.2 W. The emission designators for the amplitude modulation used for beacon and frequency modulation used for data transmission are 1.0 kHz and 20 kHz respectively. [69]

3.1 Foresail-1 satellite

The mission of Foresail-1 satellite is to investigate electron and proton precipitation processes in Earth's polar regions and neutral atoms from the Sun. A secondary mission is a technology demonstration of a Coulomb-brake method for deorbiting the spacecraft. The planned initial orbit is 700 km Sun synchronous low Earth orbit, with a planned maneuver to a lower orbit using the plasma brake [52].

Foresail-1 is a 3U form factor CubeSat carrying two main payloads: A particle telescope (PATE) to measure the radiation environment and a plasma brake (PB) for deorbiting. The plasma break is made by the Finnish Meteorological Institute (FMI), and the particle telescope by the University of Turku. The satellite development started in 2018, and a launch is planned in 2022. [52]

The satellite platform includes the aluminum structure, electric power system, UHF radio communications system, on-board computer and the attitude determination and control system. The platform is designed and built entirely in Aalto-university out of COTS components.

Because of the long planned operation time of five years, the structure has a thick aluminum layer between space and the satellite bus to mitigate radiation.

3.2 Communication system requirements

The communication system requirements specifically for the radio transmission capability for the Foresail-1 COM subsystem are defined as:

- Transmission power shall be at least 30 dBm.
- A 9600 Baud, GMSK moduation scheme shall be supported.
- Center frequency shall be 437.125 MHz.
- Occupied band shall be within the coordinated 20 kHz band at any mission temperature.
- Receiver shall be capable of receiving communication at a distance of 2200 km from the Aalto ground station.
- Communication system power consumption in transmission mode shall be less than 8 W.
- Communication system power consumption in receiver mode shall be less than 400 mW.
- Communication system shall use a single 3.6 V power rail for power.
- Communication system shall comply with regulation concerning transmission spectum use laid out by the International Telecommunication Union.

Other requirements, such as structural and interface requirements have been considered during the original design of the subsystem. The requirements listed above are ones that are to be verified by the test benches presented in this thesis.

3.2.1 Link budget

The mission nominal data rate is set at 9600 bps, and the testing is mainly done with this baud rate. Additionally, a 1200 bps data rate is explored as an option that could be utilized when operating at noisy environments or very long distances, or for possible communication issues, because of the better sensitivity at lower data rates. The 9600 bps data rate has been determined to be sufficient for the data budget of the Foresail-1 satellite. To determine the total amount of data that can be transferred per day would require the satellite orbit inclination to be known, but a minimum of about 35 minutes of communication window is required per day for Foresail-1 [49].

The link budget for a CubeSat mission requires two separate budgets, one for uplink and another for downlink. Calculating the link budget for uplink takes into account the following parameters:

- Ground station actual transmit power
- Ground station antenna gain and pointing loss
- Free space path loss
- Satellite receiver antenna gain
- Polarization loss
- Satellite receiver path losses and noise floor
- Satellite receiver E_b/N_0 required for required BER

The Aalto ground station is located at Espoo on the rooftop of a university building in Otaniemi. For the Aalto ground station, the actual transmit power is estimated to be 40 dBm and the antenna gain 15 dBi for the UHF Yagi antenna. The pointing loss is estimated to be negligible.

To communicate with the satellite, when it is just above the horizon, a line-of-sight distance of about 2200 km needs to be traveled by the radio frequency signal. It is convenient to assume free space path loss is the only factor in the attenuation of the signal at this direction as well. In reality as the beam of the transmitting antenna is grazing the horizon, some interference is possible. The free space path loss is calculated with equation (4) at a distance of 2200 km to be

$$\begin{aligned} \mathrm{L}_{2200\,\mathrm{km}}(\mathrm{dB}) &= 20\log_{10}(2200) + 20\log_{10}(437) + 32.4 \\ &= 152.1\,\mathrm{dB}. \end{aligned} \tag{21}$$

The satellite antenna gain is designed to be as isotropic as possible, so a value of -2 dB is estimated to describe the minimum gain in the radiation pattern. The polarization of the Yagi antenna at the ground station is linear and the satellite polarization is assumed to be circular, which means the polarization needs to be estimated to be 3 dB. In reality the polarization of the satellite antenna is in some directions quite linear, and much higher polarization loss could be reality. An upgrade to the ground station should include a circularly polarized antenna with selectable handedness.

The satellite's receiver's wiring loss, noise floor and E_b/N_0 requirement are included in the sensitivity of the receiver. In the design phase, the sensitivity can be difficult to estimate if the radio is a completely new design. Sensitivity is the lowest signal level the receiver can interpret with a specific bit error rate. The sensitivity of the receiver is easier and more reliable to measure than calculate. A minimum theoretical value can be estimated based on the thermal noise floor, attenuation between the antenna port and the LNA, the LNA noise figure and the E_b/N_0 required by the receiver. The attenuation between the antenna port and the LNA is estimated to be about 1 dB, where the loss in two RF switches and the filter are considered. The noise figure of the LNA is about 1 dB [46]. Since any noise at the LNA input dominates the noise figure, it should mean that the noise figure of the satellite receiver

is not much more than 2 dB. A more conservative 4 dB is used in the link budget estimate. The thermal noise floor can be calculated with equation (20). Assuming the temperature is 300 K and the bandwidth is 20 kHz, the thermal noise power is $-130.8\,\mathrm{dBm}$.

The ground station noise figure is additionally estimated to be 3 dB. The ground station noise figure has been measured and a value of about 2 dB is probably closer to the truth, but for this link budget the 3 dB is taken to include some margin in the estimate.

The thermal noise floor is estimated so that the antennas are pointing at 300 K surrounding, which for Earth is a good estimate. However, in reality, the ground station antenna is pointed at the sky, and the satellite antenna with isotropic radiation pattern is pointed about 50 % at Earth and the rest into space. Additionally, the Sun will look like a very hot target but at quite a small solid angle. Therefore, the noise is estimated to originate from an average of 300 K source. For the downlink, the worst case is when the satellite is nearly at the horizon, when half of the antenna beam is essentially pointing at ground. The average noise temperature is therefore about 150 K.

It is not clear at this point whether the MSK can be received coherently at the ground station, and therefore the E_b/N_0 requirement for both down- and uplink is taken from Figure 9 for the non-coherent FSK modulation at BER value 10^{-4}. This BER value is selected as the limit instead of a typical 10^{-5} because the addition of encoding is not taken into account at this point, and the lower BER value is seen sufficient. Reading from the figure, the reqruired E_b/N_0 is about 12 dB.

The uplink link budget with the abovementioned theoretical values and estimations, is presented in Table 5. For the downlink the link budget is presented in Table 6.

Table 5: Link budget with theoretical values for the Foresail-1 satellite with Aalto Ground Station.

Uplink link budget estimate, 9600 baud GFSK		
Ground station transmit power	40	dBm
Ground station antenna gain	15	dBi
Path loss	152.1	dB
Satellite antenna gain	-2	dBi
Polarization loss	3	dB
Total power at satellite receiver	**-102.1**	**dBm**
Receiver noise power (Thermal)	-130.8	dBm
Estimated receiver noise figure	4	dB
E_b/N_0 requirement	12	dB
Theoretical sensitivity	-114.8	dBm
Theoretical link margin	12.7	dB

Table 6: Link budget downlink with theoretical values

Downlink link budget estimate, 9600 baud GFSK		
Satellite transmit power	30	dBm
Satellite antenna gain	-2	dBi
Path loss	152.1	dB
Ground station antenna gain	15	dBi
Polarization loss	3	dB
Total power at satellite receiver	**-112.1**	**dBm**
Receiver noise power (Thermal)	-133.8	dBm
Estimated receiver noise figure	3	dB
E_b/N_0 requirement	12	dB
Theoretical sensitivity	-115.8	dBm
Theoretical link margin	6.7	dB

The link budget estimates show that there should be about 12 dB link margin in the uplink direction. For the downlink the margin is also positive at 6.7 dB.

3.2.2 Doppler effect

The relative velocity between the ground station and the satellite creates a doppler shift in the frequency. The velocity v at LEO orbit of 600 km is about 7500 km/s. If this velocity is used as the maximum velocity, the maximum doppler shift f_m in frequency for a carrier frequency f_c can be calculated using [58]

$$f_m = f_c \frac{v}{c}, \tag{22}$$

where c is the speed of light, we get

$$f_m = \frac{7500\,\mathrm{km\,s^{-1}}}{c} \cdot 437\,\mathrm{MHz} = 11\,\mathrm{kHz}. \tag{23}$$

This is the maximum possible shift in frequency for this velocity. This happens only in the case where the velocity vector of the satellite is pointing at the ground station. This is never actually the case, but this value gives the doppler shift a top boundary, or worst-case value, that can be used when estimating the actual occupied frequency band and performance under doppler shift conditions.

To correct for the error in frequency caused by the doppler shift, the satellite or ground station have to compensate for this shift. In the case for Foresail-1 this doppler shift is going to be compensated on the ground station side. The doppler effect will change the frequency of operation during the passing, and the correction has to be done either continuously or some intervals.

The satellite receiver should be able to receive transmissions that are somewhat moved from the center frequency. The bandwidth of possible operation depends on the set filter bandwidth of the transceiver. For the 9600 baud rate, the minimum bandwidth that can be set for the transceiver is about 20 kHz. For 1200 baud, the minimum bandwidth is about 4000 kHz. The transceiver can essentially find the signal if it is contained within the filtered band, which can be seen in the doppler capability measurements in Chapter 4 of this thesis. As the filter bandwidth also affects the sensitivity, there's a potential trade-off between the doppler compensation capability of the satellite and the sensitivity.

3.3 Top level radio hardware architecture

The top level diagram of the communications subsystem is shown in Figure 12. It shows the main parts of the receiving and transmission chains.

The satellite is designed to operate for 5 years, which is longer than a typical CubeSat mission length of 1-3 years. For this reason, the satellite has been designed to withstand more radiation than a typical CubeSat, while still relying mostly on COTS components. Many of the Foresail-1 subsystems are built around the Vorago VA10820 radiation hardened microcontroller, which is also the microcontroller unit in the communications subsystem.

One ideology behind the design is to increase reliability through redundancy by having two cold redundant radio sides on the circuit board. The sides are identical copies of one another nearly all the way to the smallest layout detail. The Vorago

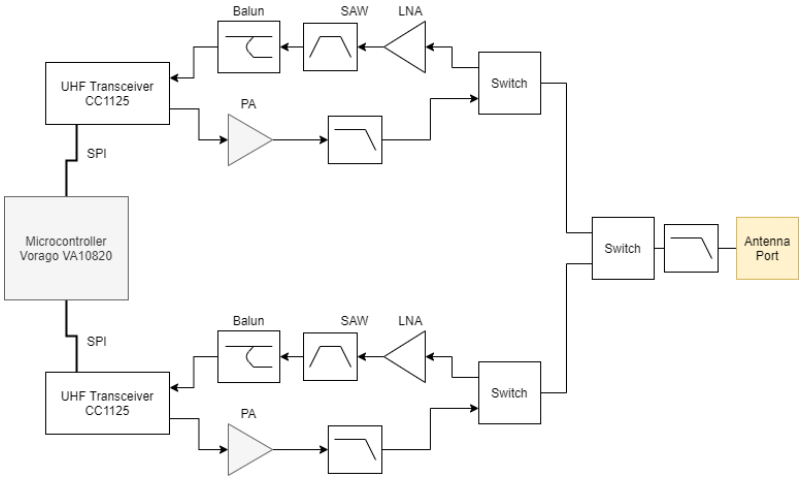

Figure 12: Foresail-1 communications subsystem top level diagram

Table 7: Radio frequency components of the Foresail-1 COM subsystem

Component type	**Component**
Transceiver	TI CC1125
Power amplifier	Qorvo RF5110G
RF Switch	Skyworks AS193-73LF
LNA	Maxim MAX2640
SAW	Golledge TA0693A
Balun	Lumped elements

microcontroller and its power regulators, and the last RF switch before the antenna are the only active devices that are not duplicated on the subsystem circuit board.

The main radio components in the communications subsystem have flight heritage from Aalto-1 CubeSat mission, including the CC1125 transceiver, the RF5110G power amplifier, the MAX2640 LNA and the RF switches [22]. The Aalto-1 satellite has survived for four years in orbit, with a design that has much less consideration on radiation shielding than what the Foresail-1 mission will have.

The Foresail-1 COM system is built around the radiation hardened Vorago VA10820 ARM MCU. There are two cold redundant transceiver sides, each connecting to the same antenna connector. Each transceiver side uses separate pins of the Vorago MCU, to ensure the loss of one side does not cause loss of the whole system.

The transceiver chip used is Texas Instruments CC1125, which handles most importantly the modulation, demodulation and frequency synthesis for the RF chain. The CC1125 communicates to the MCU through SPI interface, and optional GPIO pins. The GPIO pins can be configured to respond to events such as detection of preamble, sync word or data in RX buffer. This can be used in order so constant polling by the MCU is not necessary. [6]

The RF transmit chain includes a power amplifier Qorvo RF5110G, which has a maximum power output of 32 dBm. The gain of the PA is 32 dB, which can be

set with an external voltage. The external voltage maximum is 2.8 V, which means it requires an additional regulator. The effect of this voltage on the efficiency and power consumption is explored in one of the test benches in Chapter 4. The efficiency of the PA according to the datasheet is a maximum of 53 %. [55] The efficiency of the PA is an important factor as the PA is the most power-hungry component in the whole COM subsystem, and will essentially determine the power consumption of the whole COM system. Additionally all generated heat will have to be dissipated.

Each RF chain is split twice with AS193-73LF RF-switches, which pose an insertion loss of about 0.25 dB each. The isolation is about 28 dB. [3] The isolation is important to protect the receiver side from the transmission side high power. The absolute maximum power input for the LNA is 5 dBm [46], so a 28 dB isolation will set the maximum transmit power to 33 dBm, which is 1 dB higher than the PA maximum power output.

The matching network, filters and RX balun are made of lumped elements of 0603 size. The inductors are mostly from the Murata LQW18 series of wire wound inductors, and the capacitors are C0G rated capacitors.

The SAW filter is Golledge TA0693A. It has very narrow pass band from 430 MHz to 440 MHz and the insertion loss at 437 MHz is about 2.3 dB. The narrow pass band protects the receiver from spurious emissions in other frequencies.

The main radio components are listed in Table 7.

To make it easier to test components of the COM system, it is possible to separate the testing and characterization into the following set of components:

- CC1125 transceiver receiver + Balun
- RF5110G PA + Matching circuit or Matching circuit only
- Lumped LP+BS Filters
- LNA + SAW filter

3.4 Design simulations

The design of the Foresail-1 COM subsystem was already completed at the start of this thesis work. The original design values for the lumped elements of the radio circuit were mostly based on manufacturer datasheets and reference designs. Some linear simulations had been performed, but in the end purely ideal components were assumed in these simulations.

During the initial transmission test of the subsystem, it was obvious from the output spectrum that there was a problem. The power output was poor, while the power draw was high, and the device showed poor efficiency. The power spectrum showed there were many unexpected spurious signals at lower than carrier frequency, and the output was unstable with its frequency and amplitude. The initial emission spectrum of the Foresail-1 COM subsystem is shown in Figure 13. The marker 1 is at the correct transmit frequency. Markers 2,3 and 4 show high spurious signals at

1/4 1/2 and 3/4 carrier frequencies. There were two major issues with this version of the system. Firstly, the PA matching was poor and caused the PA to behave in a strange way, causing unexpected spurious emission in the low frequency spectrum. Secondly, a linear regulator responsible for the intermediate stage bias voltages in the PA was unstable due to too much load side capacitance causing the output power to be jumpy in the time domain.

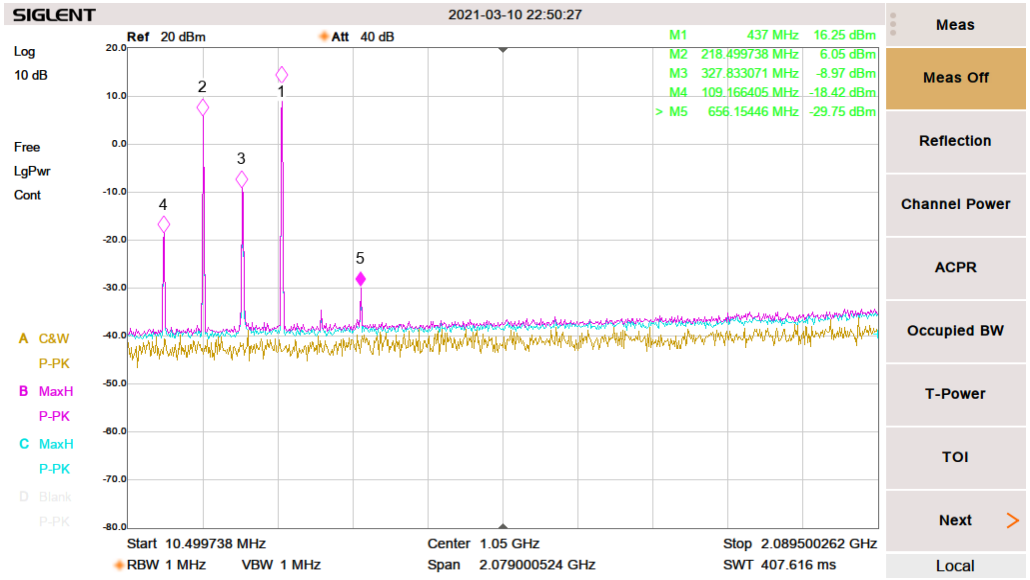

Figure 13: Output spectrum at initial matching network in Foresail-1 COM subsystem v3. Many spurious signals are present due to poor power amplifier matching. All markers (2,3,4,5) are on unwanted spurious signals.

To fix the issue, an iterative process was initially considered, but there was no good way to find out which component value changed would be helpful, and it would be total guesswork. The idea was then to simulate as well as possible all the circuitry after the power amplifier, and then measure in sections how the circuit performed.

The lumped element component values of the design were first simulated with Quite Universal Circuit Simulator (QUCS) which is a circuit simulator software resembling Microwave Office AWR. The advantage of QUCS is that it is free to use, light weight and it works on multiple operating systems. [62]

To confirm the matching network and filter design, values of the lumped elements in the power amplifier matching network, band stop filter, low pass filters and the balun were simulated.

The LNA matching was not simulated as there was a separate circuit board that could be measured. The matching network of the LNA is a single inductor, so it was felt unnecessary to simulate this. The value for this inductor is taken from Maxim Integrated application note 1759, which is for operation close to the used frequency. [45].

3.4.1 Power amplifier matching network simulation

The RF5110G datasheet provides a matching network in a reference design for 450 MHz. This was assumed to provide a close matching also at 437 MHz, and in the initial design and implementation, these values are used for the matching network.

The circuit was created in QUCS with the PA as the load with a load impedance of 2.6+j1.5. The matching network is supposed to match this load (or source) to 50 Ω. Using the values for the lumped elements given in the datasheet (L = 2.7 nH , C = 24 pF) resulted in poor matching. This can be seen from the S11 parameter in Figure 14. A high value for the S11 parameter indicates a high reflection coefficient, and a mismatch between the load and source. Also, the Smith chart shows the impedance of the circuit at 437 MHz is not close to the center of the chart. The datasheet states the "Output Load Impedance" of the power amplifier is $2.6 - j1.5$ Ohms, which is assumed to be the impedance of a conjugate matched load. Conjugate matching is required for maximum power delivery. It seemed unlikely that the PA would be designed for such poor matching. In fact making matching networks for other frequencies given in the datasheet resulted in good conjugate matching, which indicated the datasheet values were incorrect, or required specific layout.

Better values for the matching network were found using iterative methods in the simulator. It was important to attempt to find a matching network that uses an inductor value that is available, which was found to be L = 3.6 nH. The capacitance value for a near perfect match would then be C = 30 pF. The result for this new ideal matching network is shown in Figure 15

The poor matching of the original Foresail-1 prototype, it was assumed additionally to be due to the layout, which even at lower radio frequencies plays an important role. To include the layout in the simulation, it would be possible to include the microstrip traces in the QUCS simulation, but because of asymmetries in the layout at the PA output trace, it might not be possible to make a good enough model with QUCS.

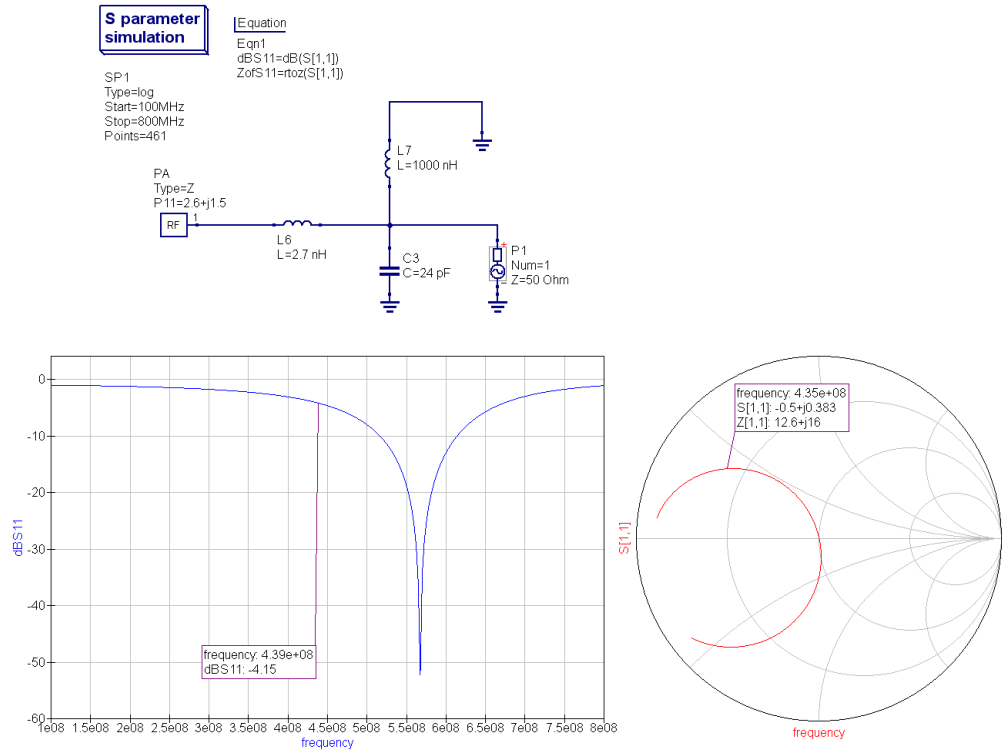

Figure 14: QUCS simulation of RF5110G matching network using ideal values taken from datasheet. The matching is very poor below 500 MHz, even though according to the datasheet this design is meant to be used at 450 MHz.

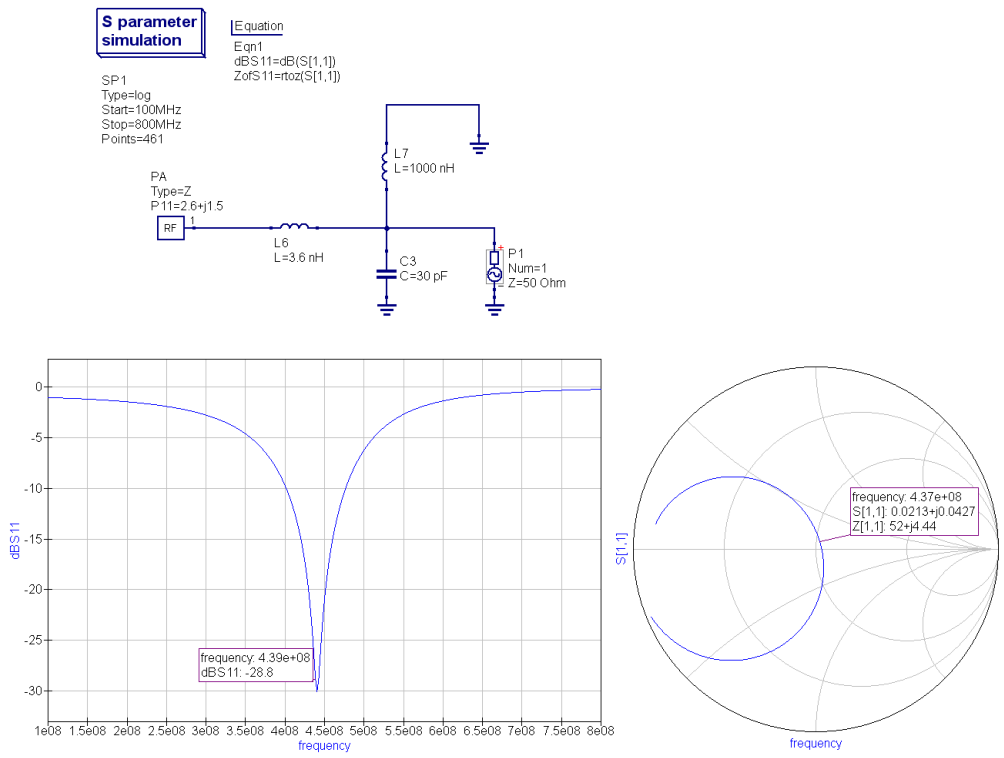

Figure 15: QUCS simulation of RF5110G matching network using refined values. Matching is good at 437 MHz.

To include the layout in the simulation, the layout was imported from KiCad to CST Studio (CST) for EM simulation. The substrate in the simulation was chosen to be lossy FR-4 with a relative dielectric coefficient of 4.3, and the metal is lossless annealed copper.

The PA output was set up as port 1, for which the impedance was also set at 50 Ohms. This way the load impedance could be read from the Smith chart. There seemed to be no simple way to give the port impedance an imaginary value in CST. The good thing about using a 50 Ohm impedance port is that the results could be verified more easily with VNA measurements. CST simulations using the ideal matching component values from QUCS showed a load impedance of $Z_L = 2.27 + j11.24$ as shown in Figure 17.

Using the Smith chart it was possible to move the impedance in the correct direction by decreasing the inductance value to the next available value. It turned out that removing the inductance completely would result in the best matching, with a capacitor value of 24 pF (L = 0 nH, C = 24 pF). The portion of the layout is shown in Figure 16. Due to CST requiring some value given for the lumped elements, the two series inductors were given value 0.01 Ohms. The resulting Smith chart and impedance at 437.125 MHz can be seen in Figure 18.

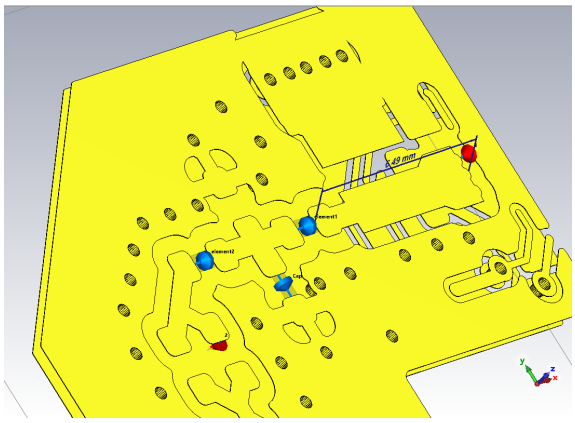

Figure 16: CST view of layout for PA matching circuit. The ports are shown in red, and the three lumped elements are shown in blue. The FR4 substrate between the layers is set to be invisible, so that only copper layers are shown.

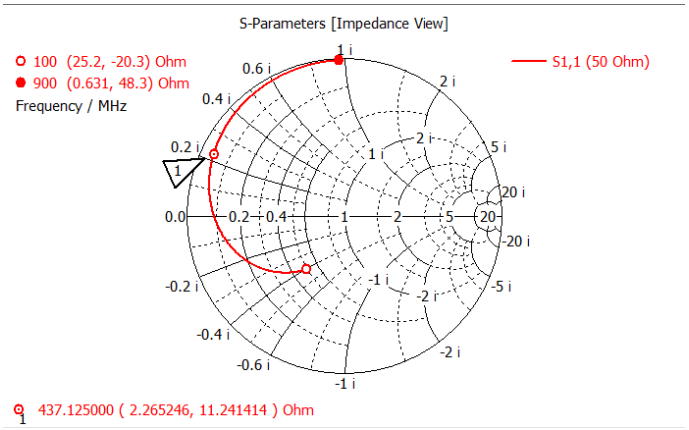

Figure 17: Smith chart for matching network using ideal component values from QUCS simulation. Load impedance seen by PA at 437.125 MHz is 2.27 + j11.24 Ohm. The matching network consists of a series inductor of 3.6 nH and a parallel capacitor of 30 pF.

The simulated load impedance is 3.26 - 1.06j Ohms. This is the impedance seen by the power amplifier at its output. The reflection coefficient resulting in the load mismatch result can be calculated assuming the PA impedance is 2.6 + 1.5j Ohms. The maximum power transfer happens when the load is conjugate matched, and the reflection coefficient can be calculated with 13 to give

$$\Gamma = \frac{Z_L - Z_0}{Z_L + Z_0}, \tag{24}$$

where Z_0 is the characteristic impedance, which can be set as the source impedance, and Z_L is the load impedance. Then the reflection coefficient is

$$\Gamma = 0.067 + 0.1j, \tag{25}$$

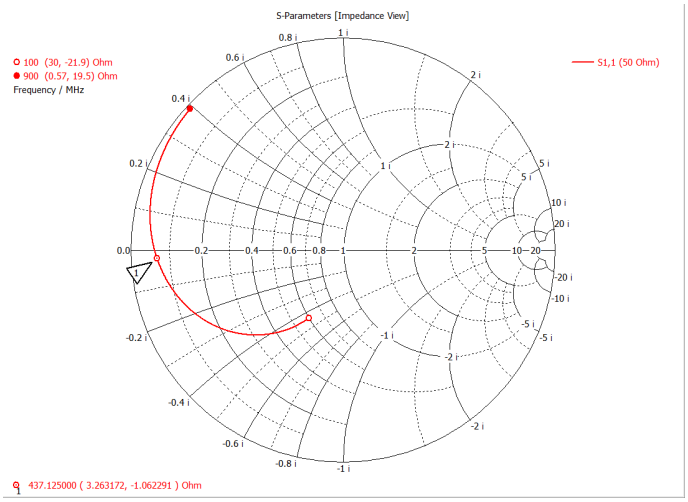

Figure 18: Smith chart for matching network. Load impedance seen by PA at 437.125 MHz is 3.26 - 1.06j Ohm. The matching network consists of two zero ohm resistors and one 24 pF capacitor. The matching is good for a 2.6 + 1.5j Ohm source.

which can be converted to reflected power percentage by

$$\text{reflected power} = 100\,\% \cdot |\Gamma^2|. \tag{26}$$

The reflected power for the simulated load is then 1.54 %.

The SWR can be calculated from the reflection coefficient using 15

$$\text{SWR} = \frac{1 + |\Gamma|}{1 - |\Gamma|}. \tag{27}$$

The calculated SWR is 1.28. This simulation would suggest the matching is good when using 0 Ohm series resistors instead of any inductors, and a 24 pF parallel capacitor in the matching circuit.

3.4.2 Transmit side filter simulation

The transmit side filter includes a band stop filter to filter out the second harmonic at 874 MHz, and a low pass filter to filter out more of the higher harmonics and possible spurious signals.

The initial values for the filters were generated with a filter designer tool, and then simulated with QUCS to verify the values with nearest physically available component values. The QUCS simulation results for the designed values is shown in Figure 19.

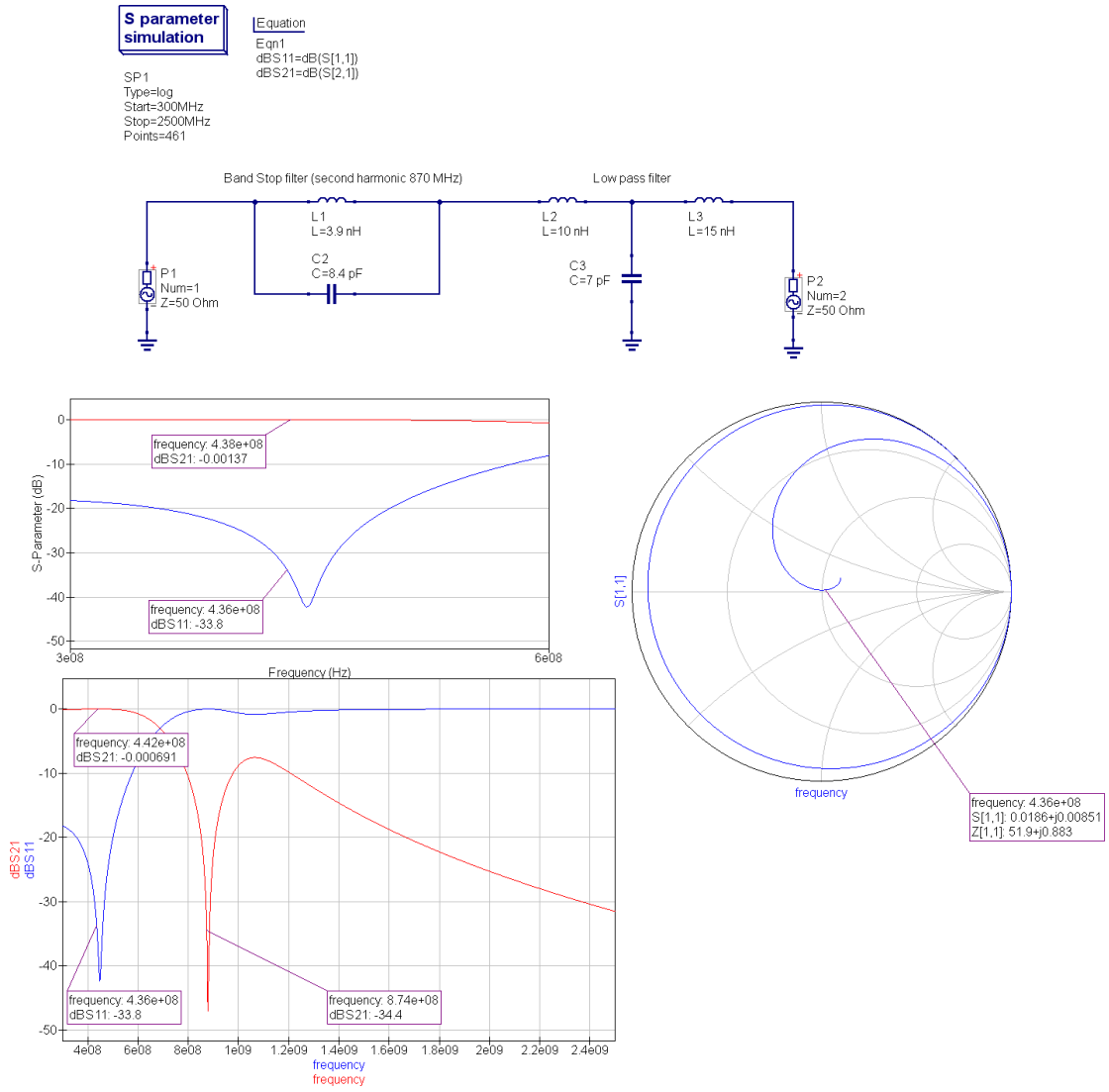

Figure 19: QUCS simulation for the transmit side filters. The band stop filter is attenuating the second harmonic at around 874 MHz, and the low pass filter works at higher frequencies. Insertion loss is negligible as S21 is nearly 0. Smith chart shows the S11 matching is very close to the center of the chart.

The QUCS simulation shows the S11 parameter in blue and S21 parameter in red. The S21 parameter at around 437 MHz show almost no attenuation, implying very low insertion loss. The band stop filter is clearly working well at 874 MHz, and shows an attenuation of over 30 dB. The third order low pass filter effect can be seen as the slow decline of the S21 parameter as frequency increases. If the band-stop filter was removed, the power at second harmonic would not be attenuated much by the low pass filter only. The power at the second harmonic would then easily be enough to cause a problem when it comes to emission outside the coordinated band.

CST simulation using the physical layout gave slightly different results as can be seen in Figure 20 as the stop band was now at a lower frequency. The insertion loss is quite good as the S21 at 437.125 MHz is only -0.08 dB. To move the block band for the band-stop filter to a higher frequency, the capacitor in the filter was tuned. This was done using a parametric sweep to find a better value for the capacitance. Changing the value from 8.4 pF to 6 pF was enough to move the stop-band to the desired frequency. Additionally the low pass filter's capacitor value was decreased slightly, from 7 pF to 6.5 pF, to provide a sightly better match at 50 Ohms. The simulation result with the adjusted values is shown in Figure 21 The Smith chart from the CST simulation for the adjusted lumped element values is shown in Figure 22.

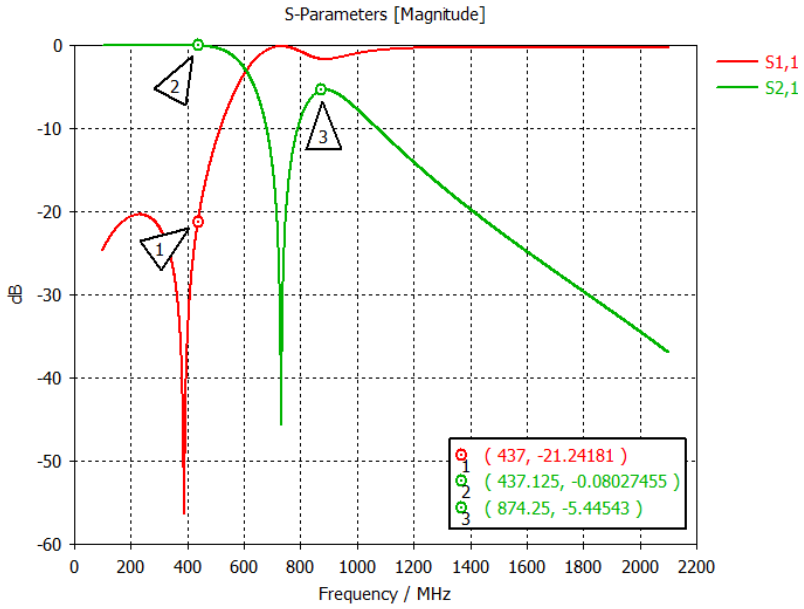

Figure 20: CST Simulation result of the transmit path lumped element filters with values from QUCS simulation. The stop band is at a lower frequency than the second harmonic.

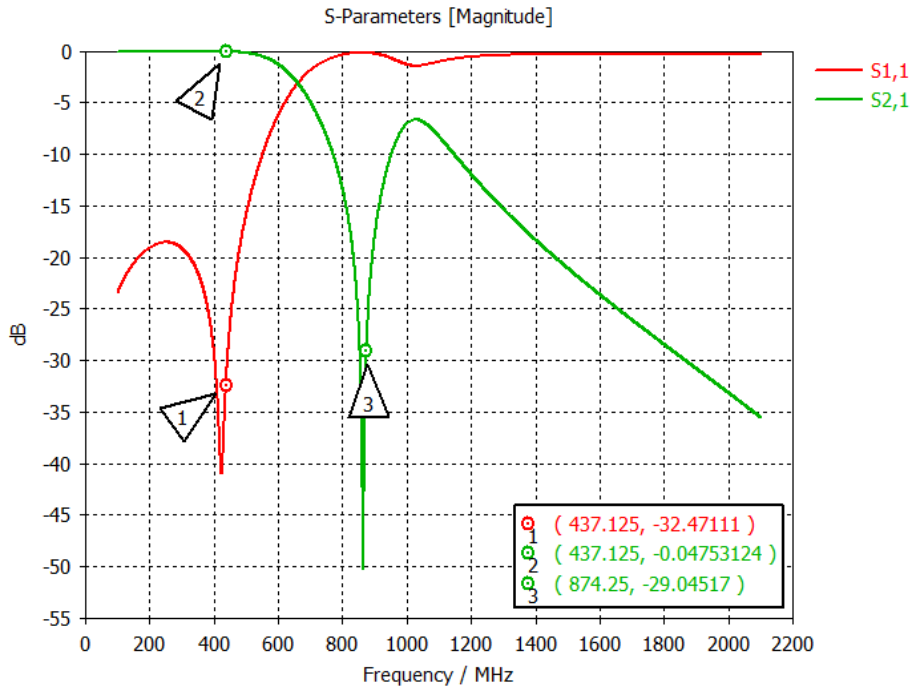

Figure 21: CST Simulation result of the transmit path lumped element filters with adjusted values. The stop band is at the second harmonic frequency and the insertion loss is very low at 437.125 MHz.

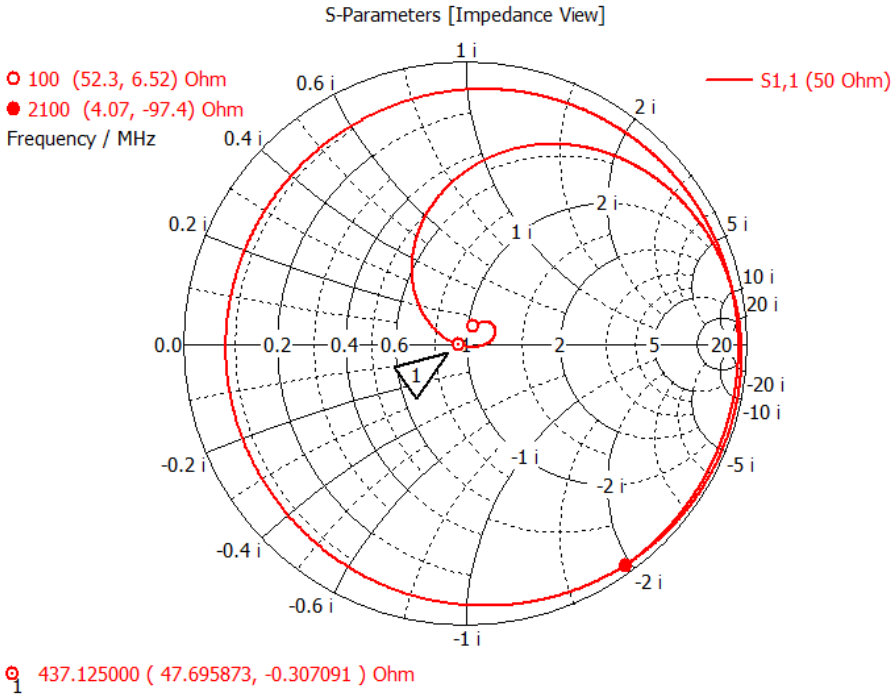

Figure 22: CST Simulation result of the transmit path lumped element filters with adjusted values. The Smith chart shows the matching to 50 Ohms is very good at the 437.125 MHz frequency.

The Smith chart shows that at low frequencies the matching is good, and the 437.125 MHz marker is nearly at the center point. A good matching means lower insertion loss and higher transmit efficiency. A good band-stop filter at the second harmonic will suppress the second harmonic that could cause a spurious transmission if not separately taken care of. The third harmonic at 1.3 GHz is also attenuated more than 10 dB by the low pass filter. At much higher frequencies, the assumption of ideal lumped elements will start to cause more and more error in the simulation result as the frequencies start to close on the self-resonance frequencies of the lumped elements.

3.4.3 Low pass filter stage

The low pass filter functions for both the receive and transmit paths. The filter further limits the spurious and harmonic transmissions at higher frequencies, as well as blocks higher frequencies from passing to the LNA, potentially causing it to saturate.

The filter design is a three stage Chebyshev low pass filter, and the QUCS simulation of the performance is shown in Figure 23.

Similar steps were taken to simulate the low pass filter in CST as in the other filter stage. This time adjusting only the capacitor values was not enough to get a great match at 50 Ohms, so the inductor value was changed from 18 nH to a lower 15 nH. Then it was possible to match the low pass filter at 50 Ohms with the help

of the Smith chart. The resulting values for the filter were (5 pF, 15 nH and 7pF) starting from the transceiver side. The resulting S-parameters are shown in Figure 24.

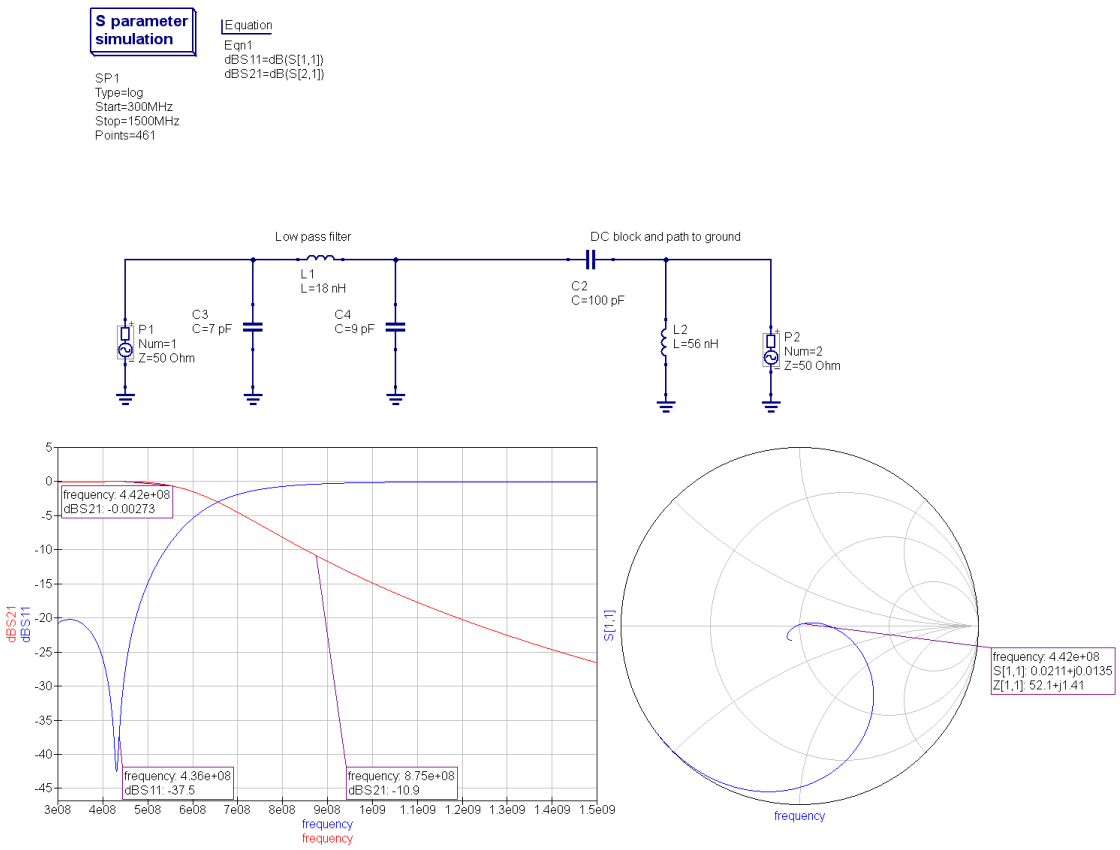

Figure 23: QUCS simulation for the low pass filter before the coaxial connector. The DC blocking capacitor and grounding inductor are included in the simulation.

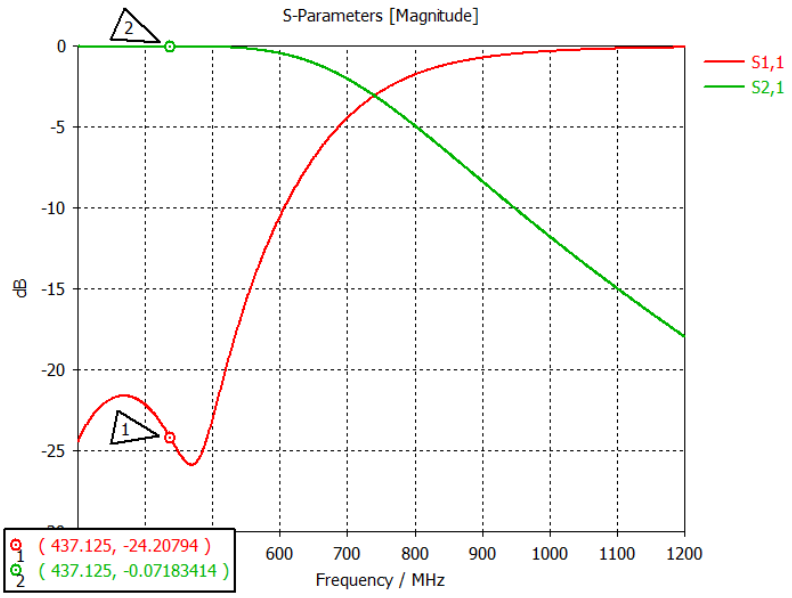

Figure 24: CST results for S-parameters S21 and S11 for the low pass filter stage. Component values from the transceiver side towards the coaxial connector are : 5 pF , 15 nH , 7 pF , 100 pF, 56 nH. The 100 pF capacitor is a DC block, and the 56 nH inductor is a DC grounding inductor.

3.5 Implementation of the radio stages

The lumped element matching circuit and filters were measured with a NanoVNA vector network analyzer. The initial values used were the ones obtained from the CST simulations. Further tuning was necessary in all three circuit elements.

The measurements were done on a second PCB, where only the lumped elements and the test leads would be soldered on to. The lack of RF test points meant that small pads of DC blocking capacitors or RF switches would need to be used to connect the coaxial cables. It was possible, but not easy or reliable, as the pads easily pull off the PCB if mechanical stress is put on them from the coaxial cables. Additionally the VNA was calibrated on calibration points made on the PCB. The calibration points were necessary to remove the error from the coaxial cables and make the results more reliable.

The image of one test setup measuring the output filter with the NanoVNA is shown in Figure 25.

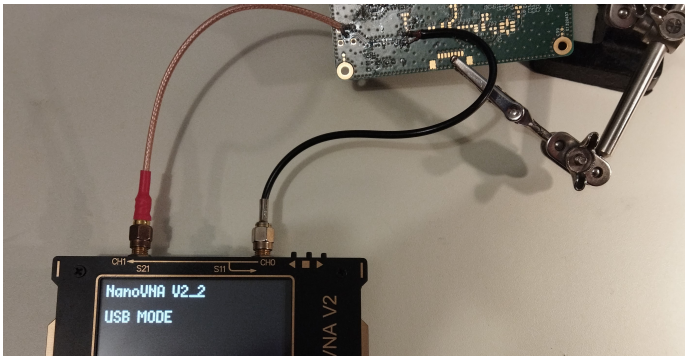

Figure 25: Measurement setup for the output filter stage. NanoVNA is connected to the computer with a USB. The two coaxial cables are soldered to the output port and the RF switch pads.

3.5.1 Low pass filter stage

The low pass filter stage was initially populated with lumped elements with values taken from the CST simulations. The Smith chart measured with the VNA showed that a small improvement could still be done by changing the component values slightly. Some of the lumped element capacitor values were iteratively tuned to end up with the Smith chart shown in Figure 26 with a very good matching at the 437 MHz frequency.

The S-parameters are shown in Figure 27. The pass band is up to a frequency of 800 MHz, where the S21 reaches -3 dB. The S11 parameter shows a very low insertion loss at 437 MHz, and the operating band is only very slightly attenuated in the filter.

The red marker in the VNA measurement graphs is at 437 MHz, and the green marker is at the second harmonic at 870 MHz.

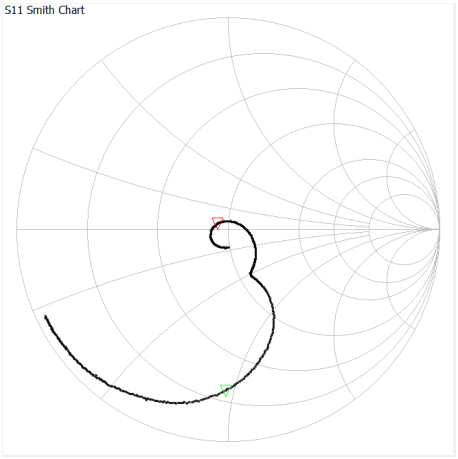

Figure 26: Low pass filter: Smith chart of the VNA measurement of the low pass filter stage. Measurement was done with a nanoVNA. Red marker is 437 MHz. Green marker is 870 MHz

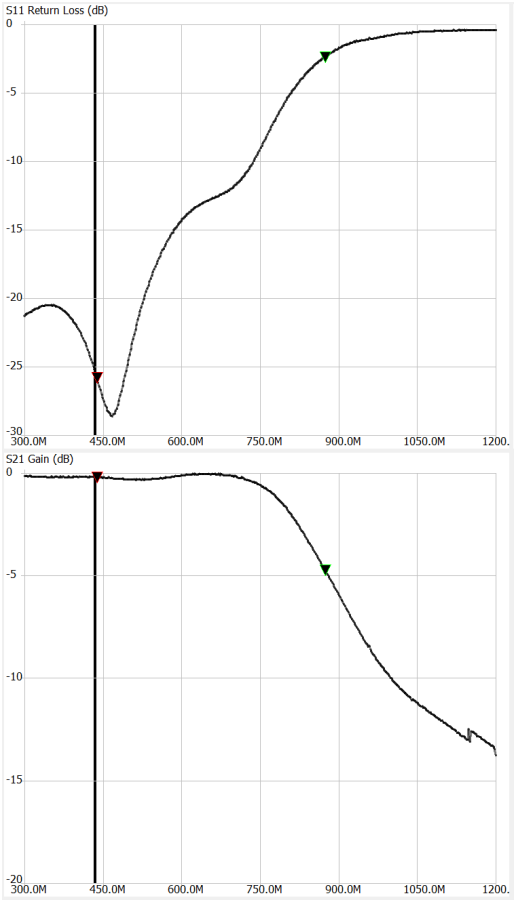

Figure 27: S-parameters for the VNA measurement of the low pass filter stage. Red marker is 437 MHz. Green marker is 870 MHz, S11 top, S21 bottom

3.5.2 Band reject filter with low pass filter

This filter was also first populated with the lumped element values from CST. The stop band was at a higher frequency than required, so the band reject filter capacitor values were tuned to a higher value. Decreasing also the capacitor of the low pass filter was required move the load impedance towards the center of the Smith chart. The original Smith chart is shown in Figure 28, and after tuning in Figure 29. The S-parameters for both the original and tuned circuits are shown in Figure 30.

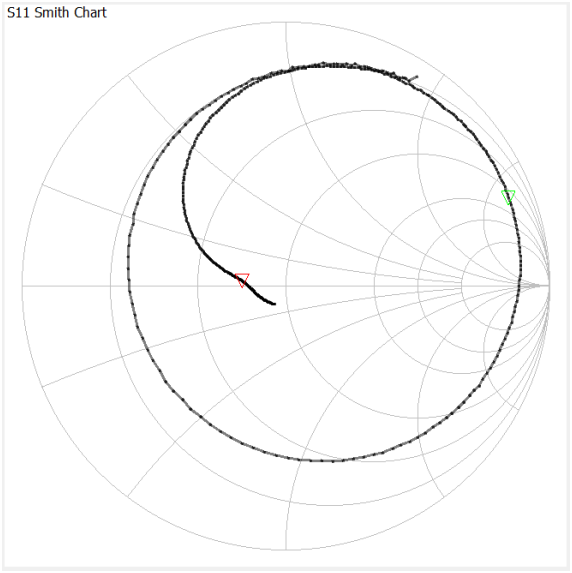

Figure 28: Smith chart of the VNA measurement of the band-stop filter and low pass filter using the values given by CST simulation. The Smith chart shows the matching is slightly off the center. Red marker is 437 MHz. Green marker is 870 MHz

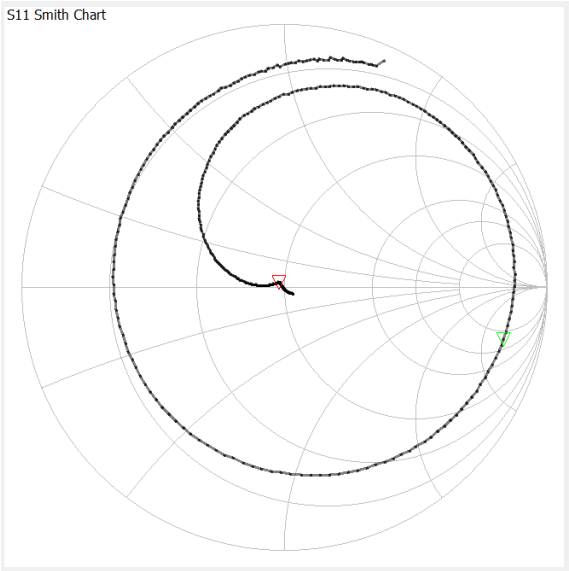

Figure 29: Smith chart of the VNA measurement of the band-stop filter and low pass filter after adjusting the capacitor values. Red marker is 437 MHz. Green marker is 870 MHz

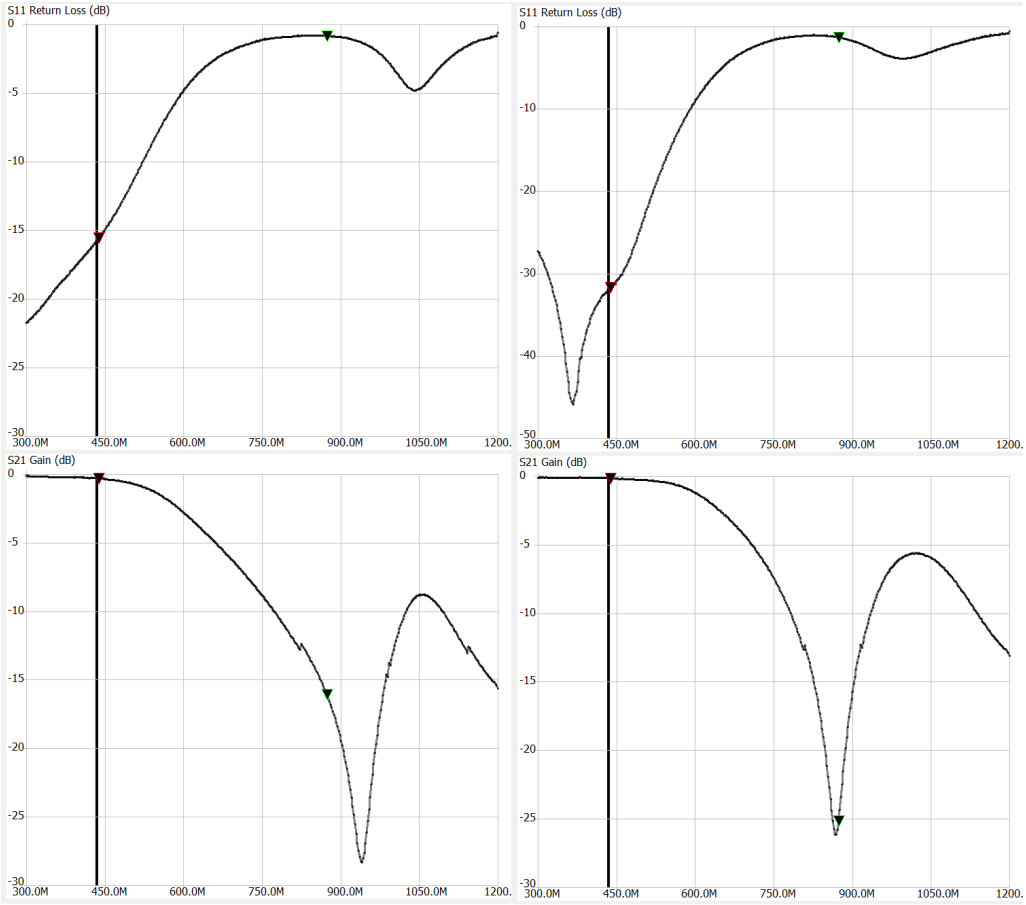

Figure 30: VNA measurement of the band-stop filter and low pass filter using the values given by CST on the left, improved values on the right. Red markers are 437 MHz. Green markers are 870 MHz , S11 top, S21 bottom

The initial values for the capacitors were 6 pF for the band-stop filter and 6.8 pF for the low pass filter. The new values are 7.5 pF and 6 pF respectively. The result with new values are shown in Figures 29 and 30 a return loss of less than -30 dB, which means the insertion loss is very low. The stop band attenuation is at 25 dB, and the low pass filter can be seen to take effect after the slight peak S21 at 1 GHz.

The matching was improved by using QUCS and simulating how a change in the capacitance value would move the marker on the Smith chart to help with the iterative process. The band-stop filter is very difficult to adjust using the Smith chart, so the S-parameters were used to tune the capacitor value of the band-stop filter. It is more convenient to adjust the capacitor than the inductance values because capacitors are typically available at very small capacitance intervals in the pF range.

The S-parameters for the band-stop filter with the low pass filter show that the original values would have resulted in a functioning circuit, with a slightly higher insertion loss than after tuning with VNA measurements. The band-stop filter attenuation at second harmonic is improved by about 10 dB.

Even though the NanoVNA given values cannot be taken as exact truth, the position of minimas and maximas in the S-parameter graphs should give indication

on the overall performance of the filters.

3.5.3 Power amplifier matching network measurement

The power amplifier matching network was measured similar to the filters. This time the target was to get the load impedance seen from the PA output port to be as close to the ideal load impedance of 2.6 - j1.5. The original VNA measurement showed a load impedance of 2 - j4.75 Ohm when using the 24 pF capacitor. Adding a 2.2 nF inductor and changing the capacitance to 22 pF we get the impedance to measure 2.57 - j2.2 Ohms with the nanoVNA. This result is shown in Figure 31.

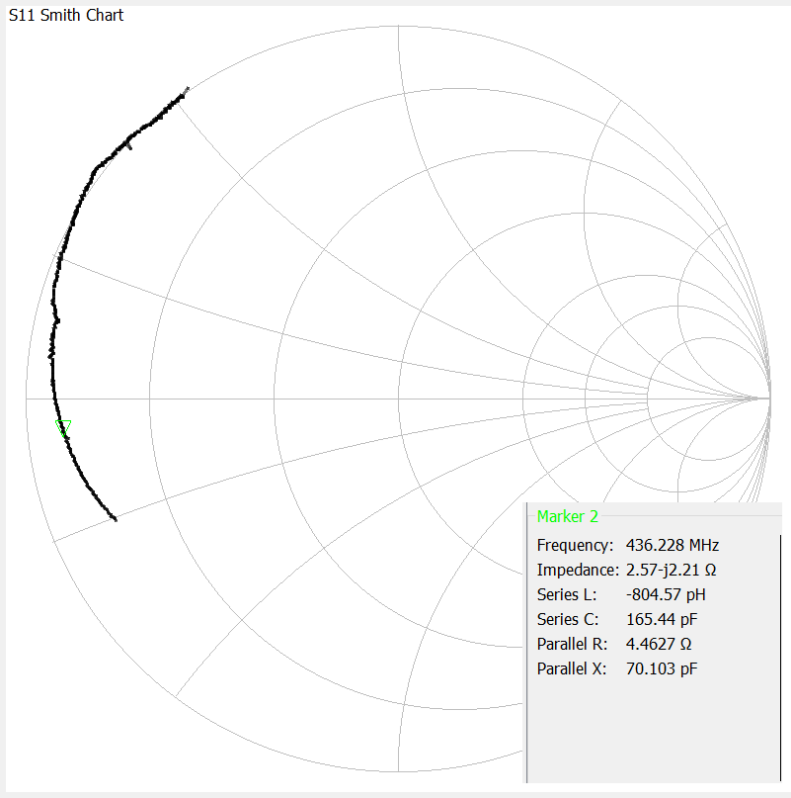

Figure 31: Smith chart and impedance value measured for the power amplifier matching circuit with nanoVNA. The result of 2.57 - j2.21 Ohms is close to the wanted 2.6 - j1.5 Ohms.

The power amplifier matching with the NanoVNA is anything but an ideal experience. It is highly likely that the result from the NanoVNA is not accurate enough to make claims on the exact load impedance seen by the power amplifier. Ideally the power amplifier would be in a separate circuit, where the layout would match the layout of the Foresail-1 COM system layout, so that the design could simply be copied from one to the other.

The described process is not really power amplifier matching, as this should be done with either a hot S22 measurement or load pull method. However the described process should give some confidence that the initial impedance seen by the

power amplifier is close enough to good matching that an iterative process could be considered for finer tuning. Additionally, the power amplifier Qorvo RF5110G has additional capacitors that are a part of the matching circuit.

3.6 Overview of the complete Foresail-1 communications subsystem

The whole Foresail-1 UHF Communications subsystem PCB layout's main sections are shown in Figure 32. A close up of the RF section only is shown in 33.

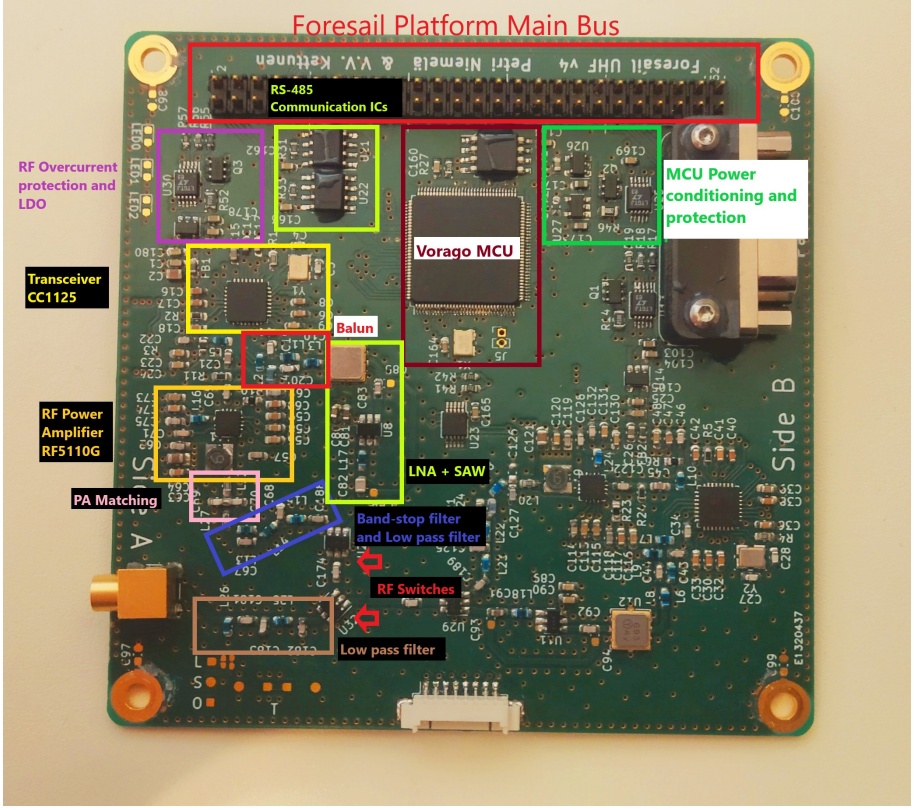

Figure 32: PCB layout of the Foresail-1 UHF Communications subsystem v4. The main sections of the "Side A" radio design is shown. A nearly identical layout is used for the Side B of the PCB.

The main components are displayed in the figure. The MCU and its power conditioning are shown in top middle and top right. These are potential single points of failure, which is why the MCU is radiation hardened and the power conditioning circuitry is automotive quality COTS components. The main communication through the satellite main bus is through an RS-485 interface, which is dual redundant. The top left corner shows the overcurrent protection for the RF side components. Additional overcurrent protection is provided from the EPS side, allowing the COM to draw a maximum current of about 1.8 A.

The transceiver, balun, PA, PA matching, filtering, LNA and SAW and the RF switches are displayed on the image. All components are soldered in the Aalto

Satellite lab. The JTAG programming connector is at the center bottom of the board.

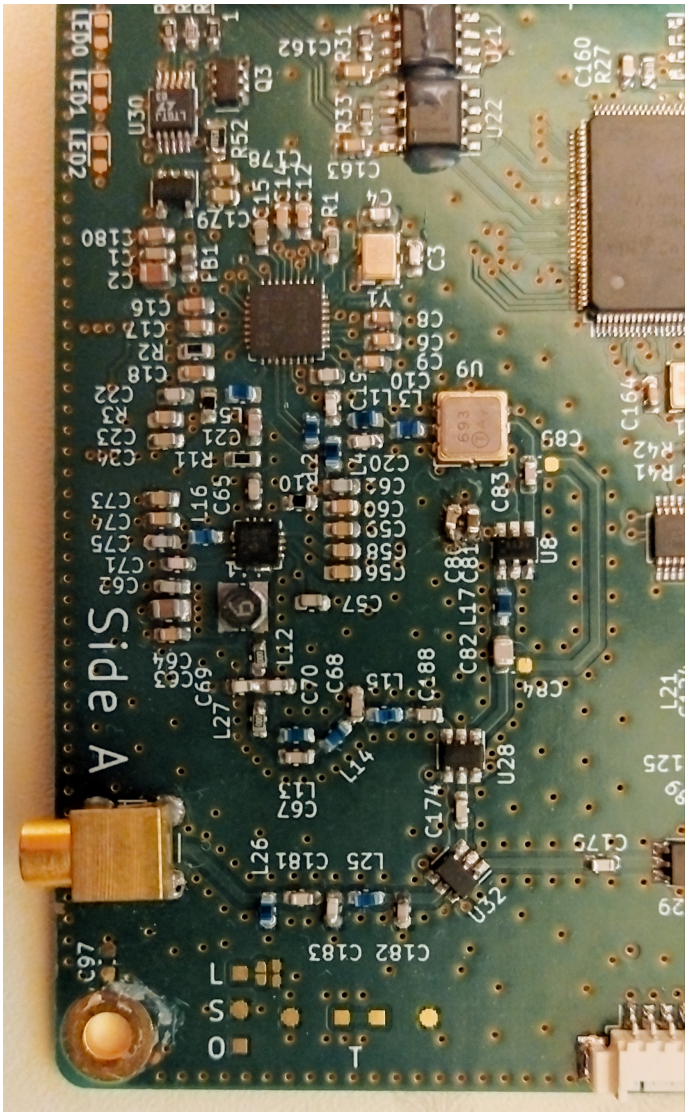

Figure 33: PCB layout focused on the Side-1 RF section.

A closer look at the RF components shows the layout and component choices. The transceiver is the IC in the center top, and the RF circuitry flows downwards in the figure into the PA. The PA requires a large inductor to provide current and block RF from entering the power bus, which is the component with the "9" or "6" on it. The pad of this inductor is considered the main reason for the matching difficulties. A different layout for the position of the inductor might have saved some trouble. The return path is shown on the right hand side, with an option to bypass the LNA and SAW with capacitors C84 and C85.

4 Radio test benches

The test bench measurements, required equipment and results for the Foresail-1 communications subsystem are described and presented in this chapter.

The tests and other important factors for the COM subsystem presented in Chapter 2 are collected into Table 8. The content is divided into five categories based on the applicability and process stage. The first category is the Design and analysis stage. These are all early stage processes, and all are applicable to the Foresail-1 COM subsystem. The second category is the implementation stage, where the tests concerning the build of the COM system and the performance. This chapter of the thesis focuses on these tests. The next category is Antenna implementation, and can be performed when both antenna system and the COM system are available. The Not applicable category has other things mentioned in Chapter 2 that are found to be inapplicable to the Foresail-1 COM system.

The Not applicable category does contain useful things like the PA protection from high SWR and RF test point use in prototyping phase. The Foresail-1 COM has however already passed these design choises. The operation in low voltage conditions is not applicable because the EPS always supplies 3.6 V to the power bus for COM. Spurious response rejection, blocking, polite spectrum access, subcarriers and duty cycle are all tests that are deemed unnecessary because of the low congestion in the amateur UHF band. The ground network compatibility refers to a commercial ground network, which Foresail-1 does not require. The adaptive power control of radio emissions is not implemented in our satellite.

The other considerations category has content that depend on firmware decisions and protocol implementation. All of these should be considered at some point. Specifically, the cessation of emissions through a telecommand should be implemented, as it is a requirement for all satellites [34].

The Design and analysis stage for the most parts have been mentioned or completed in previous parts of this thesis. For the most part the analysis and design stage of the Foresail-1 COM system had been completed at the start of this thesis. This has involved decisions on the frequencies and modulations to use involving data and link budgets. The component selection was based on flight heritage and reliability. The radiation consideration is taken into account in the design for redundancy.

The implementation stage is the primary focus of this chapter. The simulations are also placed into the implementation stage because linear and EM simulations strongly link to the iterative tuning process and performance of the COM system. The rest of the implementation stage includes tests on the power and RF performance, as well as an important tool of visual inspection that cannot be avoided when soldering the device yourself.

Table 8: A table of tests and things to consider and decide concerning the communications subsystem development, design and implementation. The "Not applicable" bracket is considered so for the Foresail-1 satellite only.

Design and analysis stage	**Implementation stage**	**Antenna implementation**	**Other considerations**	**Not applicable**
Link budget	Simulations linear	Tumbling	BER rate and frame rejection	PA protection
Ground segment analysis	Simulations EM	EIRP	Failure modes	RF test points
Component level analysis	Receiver sensitivity	Antenna measurements	Cessation of emissions	Modulation testing
Radiation consideration	Doppler	Long range test		Operation in low voltage conditions
Frequency licensing	TX power	Short range test		Adjacent channel selectivity
Modulation selection	TX power range	VSWR		Spurious response rejection
Data rates	Frequency stability			Blocking
Link protocol	Unwanted RF emissions			Polite spectrum access
	Carrier phase noise			Subcarriers
	Transient power			Ground network compatibility
	Visual inspection			Duty cycle
				Adaptive power control

4.1 Setting the operating frequency

To transmit information in the allocated radio frequency band, the radio carrier frequency must be tuned to the center of the band. In the Foresail-1 communications subsystem case, the allocated band is a 20 kHz band around the frequency 437.125 MHz. This frequency is generated by the transceiver IC internally using a phase locked loop (PLL) with the use of an external crystal resonator. The external resonator used in Foresail-1 COM is the Abracon ABM8W series 40 MHz quartz crystal resonator.

Any error in the initial carrier frequency can be attributed to the resonator circuit. The error can be corrected by adjusting the transceiver settings registers. There are two registers in the transceiver generating the transmitted frequency. First register is the main clock register that consists of three values (FREQ0,FREQ1,FREQ2), and it is set based on the desired frequency and the crystal resonator frequency. The second register (FREQOFF0 and FREQOFF1) can be used to tune the frequency to fix possible offset. The initial register values for the CC1125 transceiver IC were generated by TI's SmartRF studio 7 software, which is a software designed to help configure the TI transceiver ICs [30].

To fix the error in the carrier frequency, the transceiver was set to transmit a constant carrier wave. The carrier frequency was sent out by setting the FSK deviation frequency of the transceiver to 0, which forces both 0 and 1 to be sent at essentially the carrier frequency. Then the transceiver was set to send a continuous stream of '1's. This carrier frequency was read with a spectrum analyzer. The error in the frequency was then corrected by writing the FREQOFF-registers in the CC1125, and observing the change. The frequency offset register values can be calculated with the formula given in the user guide, which is

$$f_{VCO} = \frac{\text{FREQ}}{2^{16}} \cdot f_{XOSC} + \frac{\text{FREQOFF}}{2^{18}} \cdot f_{XOSC}, \tag{28}$$

where f_{VCO} is the output frequency multiplied by the LO divider (8), FREQ is the main frequency register, FREQOFF is the frequency offset registry and F_{XOSC} is the crystal oscillator frequency (40 MHZ). [**CC1125USER**].

From the initial frequency of 437.0678 MHz, the FREQUOFF value can be calculated with

$$\text{FREQOFF} = (437.125\,\text{MHz} - 437.0678\,\text{MHz}) \cdot \frac{2^{18}}{40\,\text{MHz}} \cdot 8, \tag{29}$$

which gives a result of 2995 or 0x0BB3 in hexadecimal format. Setting this value in the transceiver register moves the carrier to the desired 437.125 MHz frequency, which can be seen in Figure 35. The final register values are listed in Table 9.

The measurement setup block diagram is shown in Figure 34.

Setting the frequency error into this register is important so that the transceiver will operate at the correct frequency in both receiver and transmitter sides. The initial frequency error is considerable at 16 kHz. Not compensating for this error would result in transmission that is out of the allocated band.

Register name	Register value
FREQ0	0xCC
FREQ1	0x6C
FREQ2	0x57
FREQOFF1	0x0B
FREQOFF0	0xB3

Table 9: Frequency setting register values for the tested subsystem. Each individual transceiver requires its own offset calibration.

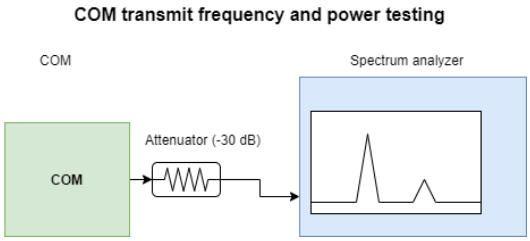

Figure 34: Test setup for frequency and power testing of the COM

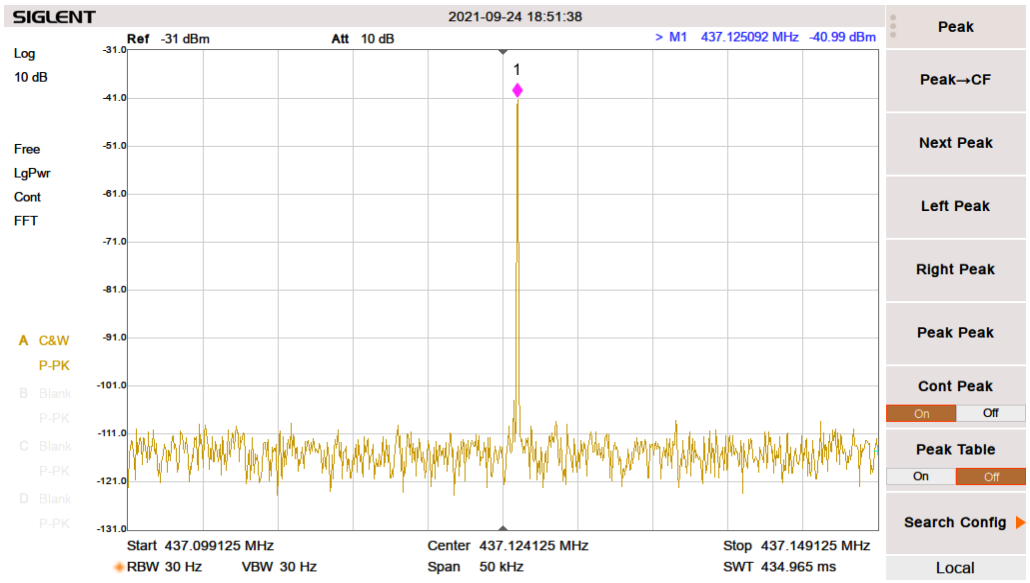

Figure 35: Carrier frequency measurement after correcting initial offset

This test and correction procedure needs to be done for both transceivers in the Foresail-1 COM, as the error is different for each side due to crystal and capacitor tolerances. This also means that each operating side of the COM will need its own frequency offset register setting in the firmware.

The error in the frequency could also be measured straight from the crystal oscillator frequency with an oscilloscope. However, the coupling between the oscilloscope probe and the resonator circuit could result in the frequency changing when the

measurement is done, giving incorrect results.

4.2 Frequency temperature dependency

The satellite temperature variation range in orbit is estimated to be between −20 °C and 60 °C. Because the frequency generation involves a crystal resonator cirucit with no thermal compensation, the frequency of the transmission could change enough to move the occupied band out of the allocated band. The crystal chosen for the Foresail-1 COM subsystem has a very good ± 10 ppm frequency stability over the temperature range according to the datasheet [54]. This temperature dependency should be visible also in the transmission frequency. Additionally, any thermal dependence for frequency generation in the transceiver is unknown, and not presented in the datasheet.

To measure the frequency shift as a function of temperature, the transmission frequency was measured with a spectrum analyzer while the Foresail-1 COM was placed into a thermal chamber. The transmission of a carrier wave was turned on at approximately 10 °C intervals, as the chamber was cooling or heating, and the position of the peak in the frequency domain was measure. It is noteworthy to mention that as soon as the transmitter was turned on, the temperature measured at the transceiver started to rise sharply. Full transmit power was used in this test, which maximized the temperature rise from transmission. The heating happens quickly as the power amplifier heating power is over 2 W. It was necessary to turn the transmission off between measurements, as cooling the transceiver to the lowest temperatures would not have been possible otherwise. The measured carrier frequency at various temperatures of the transceiver are shown in Figure 36. From the graph it is clear that the maximum frequency does not occur at the extreme temperatures, but at about 0 °C and 60 °C. The main reason for this is in the crystal that is used to generate the frequency. The temperature dependency of the transmit frequency follows that of the crystal resonator chosen for the circuit. The ABM8W oscillator datasheet shows that an approximate maximum 10 ppm deviation is to be expected from the frequency at 25 °C within the temperature range of operation. A 10 ppm deviation in either direction translates to a frequency shift of ±4.37 kHz. The measured shift is about half as large as the datasheet maximum.

The frequency deviation maximum from the measurement minimum and maximum frequencies is

$$\begin{aligned} \Delta f &= 437.1082\,\text{MHz} - 437.1043\,\text{MHz} \\ \Delta f &= 3.9\,\text{kHz}. \end{aligned} \tag{30}$$

This measurement was taken without correcting the initial frequency error, as is clear from the measured frequencies, but this has a very small effect for the actual result of this test.

It should also be noted that the ETSI standard instructs to measure the frequency at the maxims [21], and use these measurement results as the frequency range the device operates in. There is an underlying assumption of a linear frequency dependency, which is not true in the case of most crystal resonators used outside of

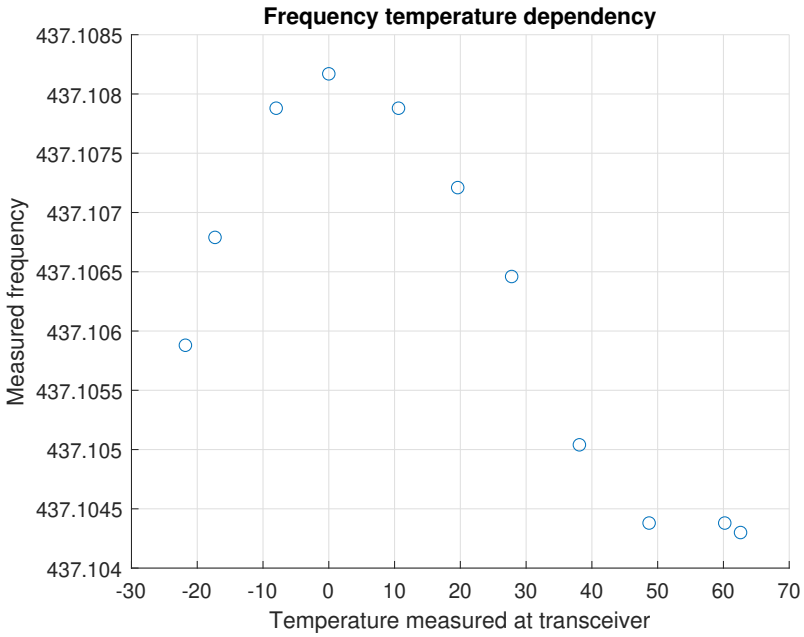

Figure 36: Frequency dependency on temperature. Temperature is measured at transceiver.

a temperature compensated crystal oscillator (TCXO). Therefore, measuring the full thermal operation range should be conducted instead, as was conducted here.

4.3 Power consumption and efficiency

The power consumption of the Foresail-1 COM subsystem is measured in two different operation modes, the transmission mode and receiving mode. Only one of the physical radio sides is turned on at any time. The measured power consumption of the subsystem when both RF sides are switched off, and when one side is in RX mode, and a typical TX mode is shown in Table 10.

The measurement was done by measuring the voltage of the power supply and the current draw with multimeters, and the output power with a spectrum analyzer. The COM subsystem was set to transmit a CW signal, and the peak power was measured with the spectrum analyzer channel power measurement tool. Generally, a spectrum analyzer is not the best tool for absolute power measurement, but the used spectrum analyzer has a relatively good absolute power accuracy of 0.7 dBm [61]. Additionally, a power meter was used to confirm the maximum power output, and it agreed with the spectrum analyzer result. Therefore, it can be assumed that the spectrum analyzer accuracy in this measurement is actually much greater than the minimum specified in the datasheet. The attenuation of the cabling was measured to be 0.8 dB, and additionally an SMA attenuator of 30 dB was set in series to protect the spectrum analyzer from high power input.

The results show that turning on the receiver will consume only about 80 mW in total. A total subsystem power draw at receive mode is quite low at around 300 mW. This is good for the power budget, as the receiver is set to be on at all times.

Table 10: Table of power consumption of the Foresail-1 COM subsystem v4 at different modes. The power amplifier second stage regulator voltage used here is 2.6 V.

Mode	Current draw [mA]	Power draw [mW]	Power (10 % margin) [mW]
Idle	56.6	203.8	224
RX	79	284.4	312
TX	1330	4788	5266

The nearly 5 W transmission mode power is considerable, and for a constant transmission this is too high for almost any CubeSat power budget. As the transmission mode is on only during the communication window and even then it is on only some of the time because of the time-division duplexing scheme, it is not a power budget problem. The power consumption however shows that even with an ideal efficiency of 50 % we end up having a small component with a 2.5 W heat loss in the circuit.

Table 11: Power output when using 2.6 Volt power amplifier gain stage voltage. This shows the gain is about 33 dB, and maximum efficiency is achieved at -3 dBm input power.

TRX power (dBm)	Current (A)	TX power (dBm)	Efficiency (%)
-11	0.63	24.37	14.90
-6	0.98	28.84	24.73
-3	1.16	29.9	26.10
0	1.33	30.36	24.94
1	1.35	30.37	24.59
2	1.37	30.39	24.31
3	1.38	30.39	24.12

Because most of the power is consumed when the system is in transmission mode, there could be a situation where the satellite is required to limit the amount of transmit time for power budgeting reasons. For data budget requirements, it is however necessary to downlink a certain amount of data every day, and operate the satellite every passing.

The power amplifier gain can be controlled by selecting a voltage for the first and intermediate stage of the multi stage amplifier. Two linear regulator voltage values were tested to see if this makes a difference in the efficiency or power consumption. The output power of the transceiver was controlled from its registries, and the transmitted power of the subsystem was measured. The results of the 2V gain stage is shown in Table 12. The results for the 2V6 gain stage voltage is shown in Table

Table 12: Power output when using 2 Volt power amplifier gain stage voltage. Efficiency is estimated from total power consumption.

TRX power (dBm)	Curent (A)	TX power (dBm)	Efficiency (%)
-11	0.08	-40	0.00%
-6	0.08	-37	0.00%
-3	0.09	-30	0.00%
0	0.19	7.7	1.36%
1	0.3	15.5	4.29%
2	0.52	22.2	10.24%
3	0.69	24.8	13.53%
4	0.84	26.7	16.87%
5	1.06	28.7	20.80%
6	1.15	29.3	21.89%
7	1.23	29.77	22.71%
8	1.28	30.13	23.65%
9	1.3	30.2	23.65

11. The significance of the gain stage voltage to the efficiency or power consumption is minimal in the performed tests. However using the 2 V regulator at the gain stage makes the desired 30 dBm power output barely reachable with the transceiver output of 8 dBm. The power amplifier maximum input power according to the datasheet is 13 dBm, but it would be better to leave some margin to this absolute maximum value. The tested maximum output power from the transceiver was 9 dBm, but for the test with a 2.6 V regulator, the amplifier clearly saturated already at 0 dBm output power.

The significance of the gain stage voltage to the output efficiency and power consumption was negligible. The output power of the transceiver should however be adjusted to ensure maximum output efficiency and power. The maximum efficiency of the power amplifier is reached when it saturates. If there would be a need for adjustable power output, for example for regulatory reasons, then it would be easiest to choose a lower gain stage regulation voltage. The efficiency is however reduced greatly when the power amplifier is not operated near saturation.

The efficiency shown is calculated by removing the idle current draw from the total power draw. Therefore, the efficiency shown is not the power amplifier efficiency, but the whole transmit side efficiency including any wiring losses. The maximum efficiency of 26 % is nevertheless quite low compared to the maximum possible efficiency. The main factor is assumed at this point to be the matching network of the power amplifier, however some iterative tuning of the power amplifier matching components showed no improvement in the efficiency. Considering the losses in the filter stages, switches and cabling between the spectrum analyzer it can be estimated that a minimum of 0.7 dBm is lost.

4.4 Effective isotropic radiated power

The goal for the effective isotropic radiated power test is to estimate the total RF power radiated by the Foresail-1 COM subsystem during transmission in either polarization direction.

This is an important characteristic for possible regulatory purposes and confirmation of the values for the link budget calculation. The effective isotropic radiated power (EIRP) includes the antenna gain and polarization, as well as any losses between the radio subsystem and the antennas. [58]

$$\mathrm{EIRP}_{dB} = P_T + G_A - L_C \text{ dB}, \tag{31}$$

where P_T is the measured transmitted power, G_A is the antenna gain and L_C is the losses between the subsystem and the antennas.

Since this test bench is performed only in conducted mode instead of radiated mode, values for the antenna gain and cabling losses need to be either estimated from simulation or other measurements. Foresail-1 uses four monopole antennas combined in a phasing network to create a circular polarization pattern with a nearly isotropic radiation pattern. The antenna pattern was simulated and shows an absolute maximum gain G_A of 3.25 dBi and a minimum gain of approximately -2 dBi [27]. The simulation does not separate the horizontal and vertical polarization.

The phasing network is built using COTS splitter ICs with a reported attenuation of approximately 0.3 dB. Each path goes through two splitters resulting in an attenuation of 0.6 dB. There are also lumped element phase shifters and antenna matching components, which introduce some attenuation. The resulting value of $L_C = 0.8\,\text{dB}$ is estimated as the loss for the whole path.

The test bench for the effective power is described in Figure 34 and is the same as used in all transmit power measurement testing. The value of the attenuator is a minimum of 10 dB for the spectrum analyzer to prevent damage to its front end.

A CW transmitted power measurement is shown in Figure 37. The measurement shows the occupied channel bandwidth measurement in CW mode, and constains 99 % of the power. The figure shows the radiated power is 20.30 dBm, when a 10 dB attenuator is used at the output. After adding the effect of the attenuator to the measured value we get a transmitted power of 30.30 dBm, when assuming no cable losses at this test.

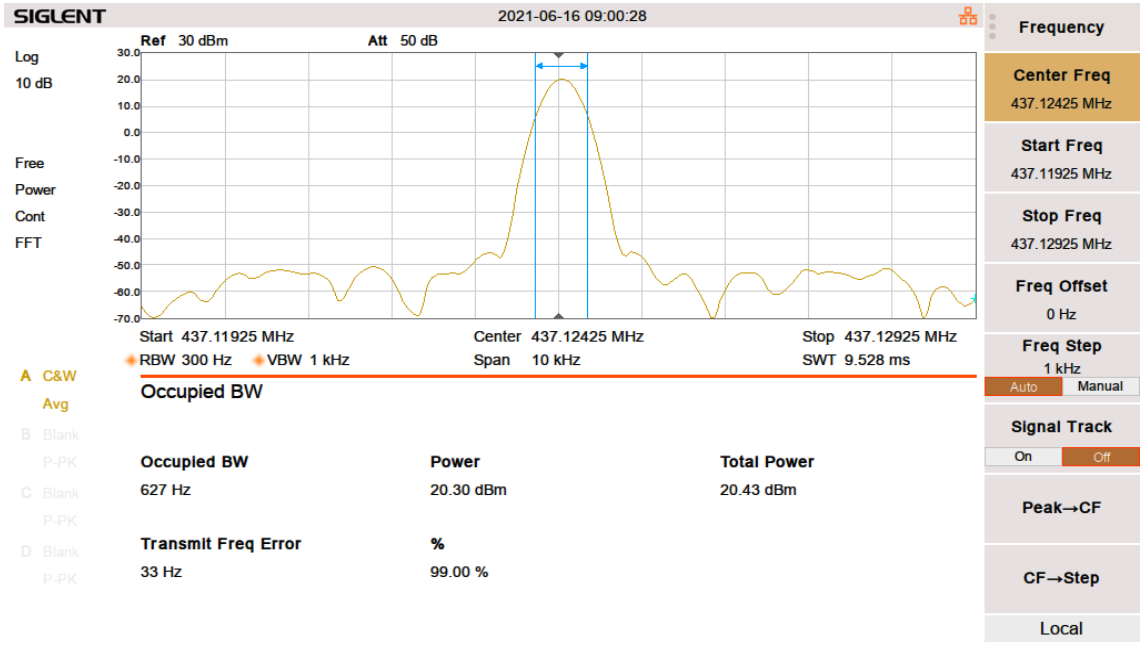

Figure 37: Effective transmitted power measurement result in CW mode. A 10 dB attenuator is placed between the spectrum analyzer and the DUT.

Because the wanted directionality of the antenna is completely isotropic, the effective radiated power minimum and maximum are evaluated here. This gives the limits that can be used in the link budget estimation as well as possible regulatory requirement. The effective isotropic radiated power values for the minimum and maximum cases using the previously determined antenna gains and path losses are shown in Table 13.

The EIRP minimum value should be used in the link budget calculation, as no pointing capability for the satellite can be assumed. The EIRP shown here is not for any specific polarization, but the absolute value for the pattern. The minimum value occurs in the region of the radiation pattern where the radiation is practically

Table 13: Effective Isotropic Radiated Power for Foresail-1 satellite using measured transmit power, simulated antenna gain pattern and estimated path loss.

EIRP Maximum	32.75 dBm
EIRP Minimum	27.5 dBm

linear, at the XY axis of the frame.

4.5 Occupied bandwidth

The occupied bandwidth measures the bandwidth containing 99% of the transmitted power. The operating channel according to the allocation to Foresail-1 is a 20 kHz band around 437.125 MHz, and the occupied band needs to be contained within this.

The measurement was done with the same measurement setup as the power measurement, by using an attenuator and a spectrum analyzer. The Siglent SSA 3021X Plus has a function to measure the occupied channel width, and it is used here. The Foresail-1 COM subsystem is set to transmit a modulated signal.

The transmitted signal's measured occupied bandwidth is shown in Figure 38. A 30 dB attenuator is used in this case. The value of the attenuator does not change the occupied bandwidth. The spectrum analyzer is set to hold the maximum value and the measurement is run for about a minute. The transmitted signal is pseudo random 64 byte long hexadecimal packet being sent continuously to maximize the transitions between the two bit values. Sending a signal with a repeating "01010101" occupies a narrower band due to the GFSK modulation scheme, so a more random message was generated for this measurement.

The test result confirms that the occupied band resides within the allocated band, in a 9.7 kHz band.

The end result also has to account for the possible temperature caused shift in frequency. The measurement result for the frequency shift is added to the occupied bandwidth to resulting in a wider possible occupied bandwidth. With the frequency shift of $\Delta f = 3.9$ kHz the resulting occupied band width becomes 13.6 kHz. This is still well within the allocated 20 kHz bandwidth. There is even plenty of room for additional doppler shift.

Comparing the result to the calculated ITU occupied bandwidth in Chapter 2 of this thesis, we find that the occupied bandwidth is about 10 % higher than the calculated MSK occupied bandwidth, but the estimate is very close. Using Carson's rule would be too pessimistic by almost 50 %.

4.6 Adjacent channel power

Adjacent channel power is power that is being transmitted into the neighboring channels of the allocated channel.

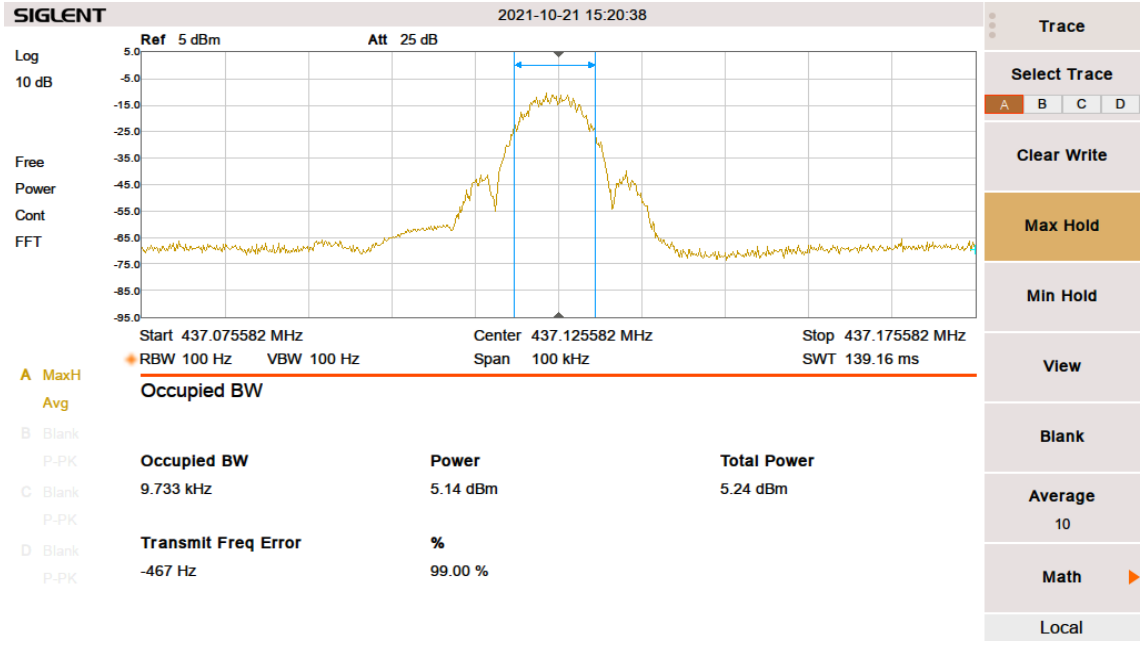

Figure 38: Occupied bandwidth measurement. Occupied bandwidth is 9.7 kHz. Test signal is pseudo random and the spectrum analyzer is using max hold function with a 100 Hz resolution bandwidth. A 20 dB attenuator is between the spectrum analyzer and DUT.

The measurement result is shown in Figure 39. The figure shows that the highest intermodulation peaks also reside within the channel. More intermodulation peaks appear as the resolution bandwidth was lowered for this measurement from 300 Hz to 100 Hz. This has no effect on the result, as the spectrum analyzer channel power function integrates the power over the channel.

The channel width is taken according to the ETSI 300 220-1 instructions to be 0.7 occupied channel width. In this case the 20 kHz OCW results in 14 kHz side channel width.

The power level is approximately -52 dBc for each of the adjacent channels. ETSI 300 220-1 gives a limit power level under normal test conditions to be -37 dBm integrated over 0.7 OCW.

Adjacent channel power measurement is not applicable or necessary for a CubeSat in the amateur UHF frequencies. The adjacent channel domain is covered by the out-of-band emission domain.

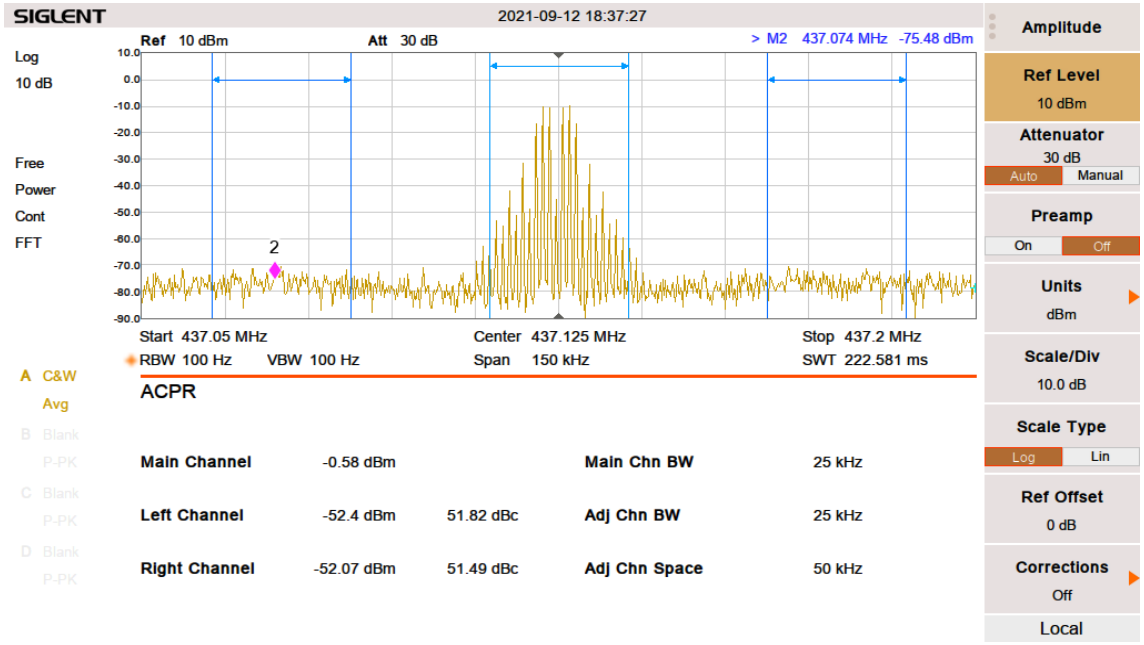

Figure 39: Adjacent channel power measurement. The measurement shows some phase noise in the adjacent channels, with a total channel power of -51.5 dBc on each side.

4.7 Transmitted out of band emissions

The out-of-band emission domain is the area immediately around the operating channel. The emission in this domain is dominated by the modulation process. The region outside this band is called spurious domain. The spurious emissions are caused by other than modulation processes. [21]

The OOB domain emission spectrum limits are given in the ETSI-300-220 as an emission mask and a table of values. The emission mask given by the standard is presented in Figure 6.

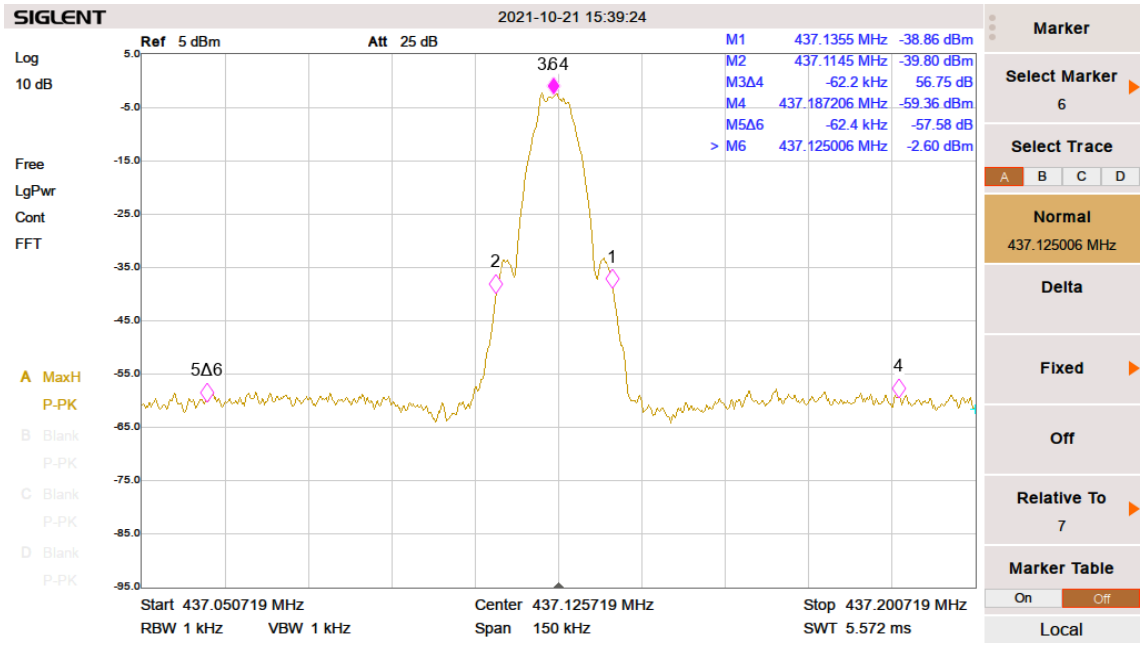

Figure 40: Measured out of band emission spectrum.

The measured emission in the OOB domain is presented in Figure 40. The spectrum is measured by taking 100 average values during the transmission of a repeating pseudo random packet. The measurement resolution bandwidth is set to 1 kHz for easy comparison with the emission mask.

Markers should be set to the edges of the operating channel (437.115 kHz and 437.135 kHz) but then moved closer to the carrier frequency by 2 kHz to take into account the thermal frequency shift. Similarly markers should be set at $f_c \pm 2.5 \cdot \mathrm{OCW}$ (437.075 kHz and 437.175 kHz). At this distance the thermal uncertainty makes little difference.

The emission mask requires values of 0 dBm and −36 dBm from the two marker positions respectively.

In this test the attenuation between the Foresail-1 COM and the spectrum analyzer is estimated to be 30.5 dB taking into account both the attenuator and the cabling losses. The markers are unfortunately misplaced in the figure, but the values for the points of interested can be estimated from the graph. The resulting values are presented in Table 14.

Table 14: Out of band emission mask and measured values comparison. The powers are taken with 1 kHz resolution bandwidth.

Frequency	Measured power (dBm)	Allowed power (dBm)
437.117 MHz	-2	0
437.133 MHz	-3	0
437.175 MHz	-38.8	-36
437.075 MHz	-37.1	-36

The measurement results show that the measured power in the OOB domain is within the allowed emission mask, but there is not much margin in the outer regions of the band. It seems that the output power close to the transmission channel is well contained and there is no problem with generated emission outside the channel from the modulation process.

4.8 Transmitted spurious emissions

The spurious domain covers the domain that is everywhere outside the out-of-band domain. Essentially the rest of the radio frequency spectrum. The limit to the measured frequency band is only limited by the equipment available. The ETSI standard gives an emission mask for the spurious domain and is shown in Chapter 2 in Figure 8. The measurement result for the region near the operating frequency is shown in Figure 41.

The points of interest from the emission mask are listed in Table 15 representing points at $f_c \pm (4 \cdot 20\,\text{kHz})$ and $f_c \pm (10 \cdot 20\,\text{kHz})$

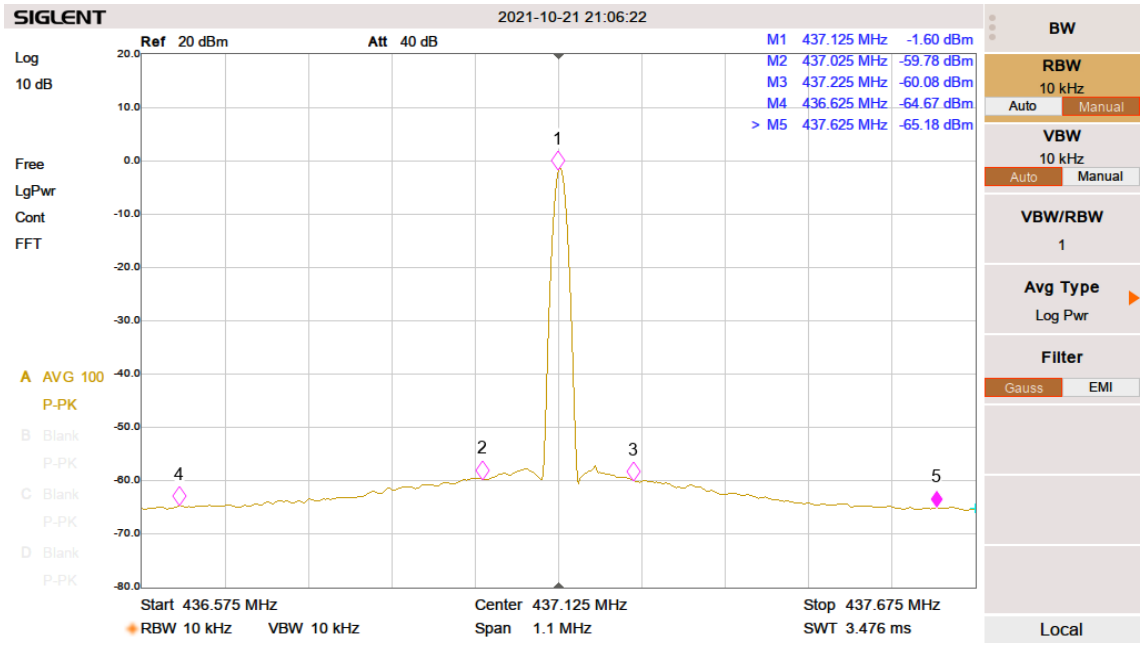

Figure 41: Measured spurious emission spectrum near the operating frequency.

Table 15: Spurious domain emission mask and measured values comparison. The powers are defined with 10 kHz resolution bandwidth.

Frequency	Measured power (dBm)	Allowed power (dBm)
437.045 MHz	-28	-26
437.205 MHz	-28	-26
436.025 MHz	-32	-36
437.325 MHz	-32	-36

The transmitted power for the rest of the spurious domain is measured with the spectrum analyzer maximum span. The spectrum is shown in 42. The spectrum shows no spurious signals above the spectrum analyzer noise floor. The limit for

spurious emissions is given as −46 dBm/100 kHz. This figure shows there are no significant harmonics at the output, nor are there any other spurious emissions.

The emission limit is exceeded in the domain about 200 kHz away from the center frequency. The reason could be the crystal oscillator circuitry around the CC1125 transceiver.

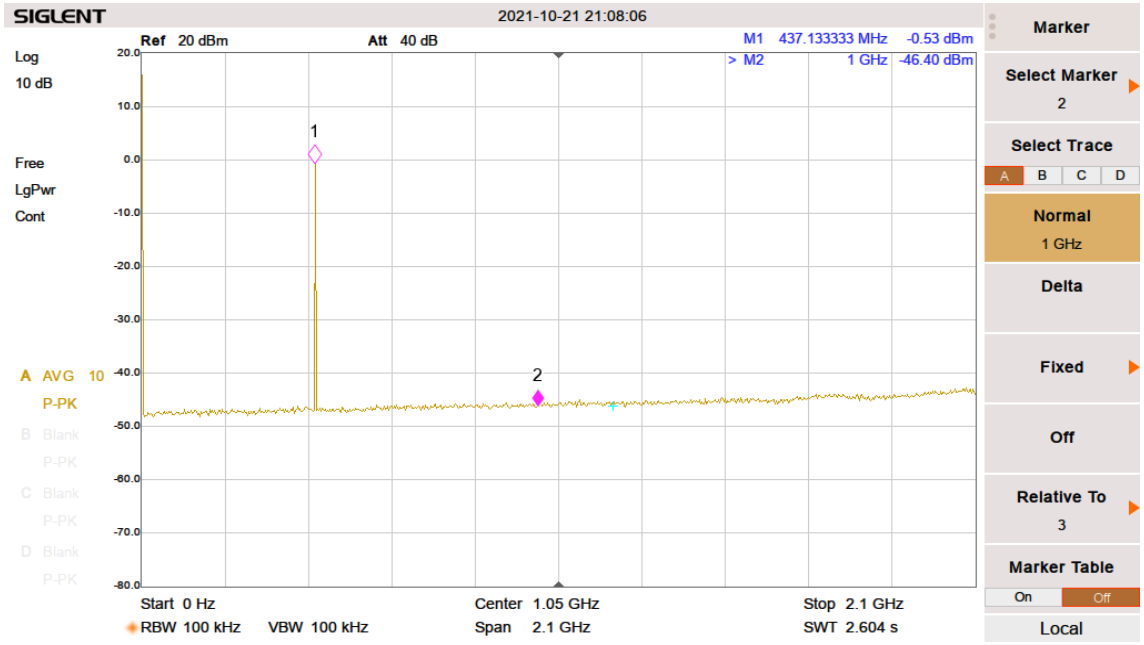

Figure 42: Transmission power in the spurious domain. There are no harmonics or higher frequency spurious emissions.

4.9 Receiver sensitivity

The receiver sensitivity was tested by transmitting constant length frames from a computer through a USRP software radio device to the Foresail-1 COM, and reading the received frames from the subsystem back to a computer through the JTAG debugging interface. The bit error rate was calculated from the difference between the sent and received bytes. No error correction scheme was used, and the data was not whitened. The frames were about 250 bytes long pseudorandom data. A minimum of 100 frames were transmitted for each measurement. The graph of measurement results is shown in Figure 44.

The physical measurement setup is shown in Figure 43. The USRP is controlled through GnuRadio, which gets the frames from a ZMQ source. The GnuRadio graph does the modulation and transmits the frames to the output port. This port is attenuated enough to reach the low required powers. The attenuated signal is divided in an RF splitter, which ensures the spectrum analyzer receives the same signal power level as the Foresail-1 COM subsystem. The excellent dynamic range, low noise floor and front-end low noise amplifier of the spectrum analyzer ensures it is able to measure the very low channel power. If the noise floor of the spectrum

analyzer would not allow measuring such low powers, it would be possible to use an external LNA or split the power before attenuating the signal.

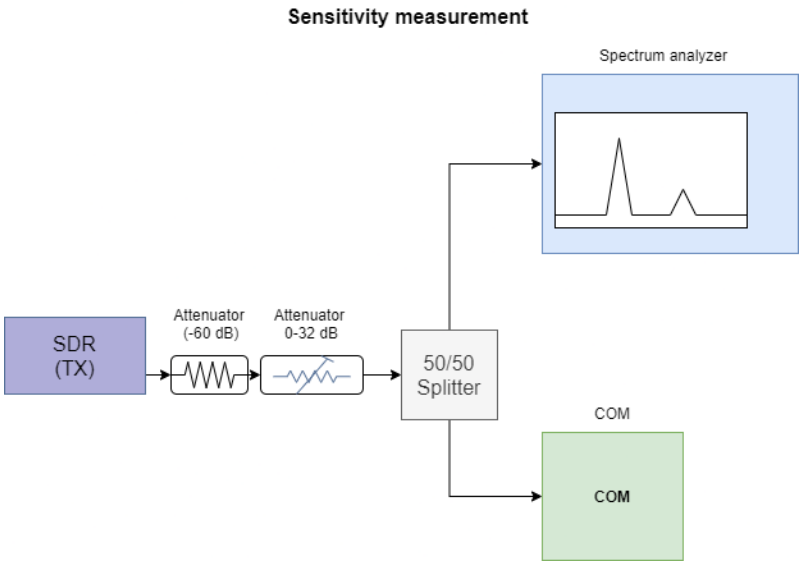

Figure 43: Sensitivity measurement test setup.

The limit for the BER was defined by requirement to be below 10^{-4}, which then allows the error correction to further improve the error rate. The channel filter width for the 9600 baud is set in the transceiver, and is set to be the minimum allowed 20 kHz. The BER is shown to quickly increase at the point where the measurement results start to show errors, as the received power is decreased. This means that this measured sensitivity value is quite a strong limit to the reception capability. The result of -106 dBm is a decent value and leaves some margin in the link margin. However theoretically the receiver should be able to do better.

Using 1200 baud would allow narrowing the transceiver's filter bandwidth to about 4 kHz, which would increase sensitivity even more. The filter bandwidth is kept at 10 kHz for the 1200 baud test, because a wider band allows the receiver to find the signal at this wider band.

4.10 Doppler capability of receiver

The receiver sensitivity was measured for different transmit frequencies around the center frequency. The result of the test is shown in Figure 45. The result shows that the receiver performs equally well within about a 10 kHz band. The test setup had the nominal baud rate of 9600, and the CC1125 filter was set to the minimum bandwidth of about 20 kHz. Similar test was performed for the 1200 baud rate transmission with the CC1125 filter set to about 4 kHz bandwidth, and the result resulted in higher sensitivity but poorer doppler capability, as the operational band ended up much narrower.

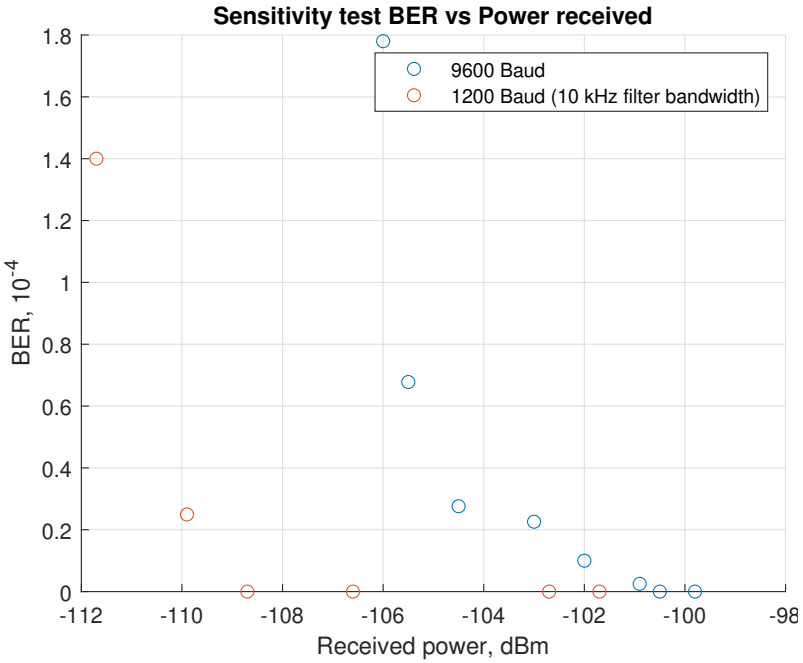

Figure 44: Sensitivity measurement test results. The sensitivity of the receiver is where BER is below 1 e-4. Two baud rates were measured, and the results shows 1200 baud increases sensitivity to about -111 dBm compared to -106 dBm for 9600 baud

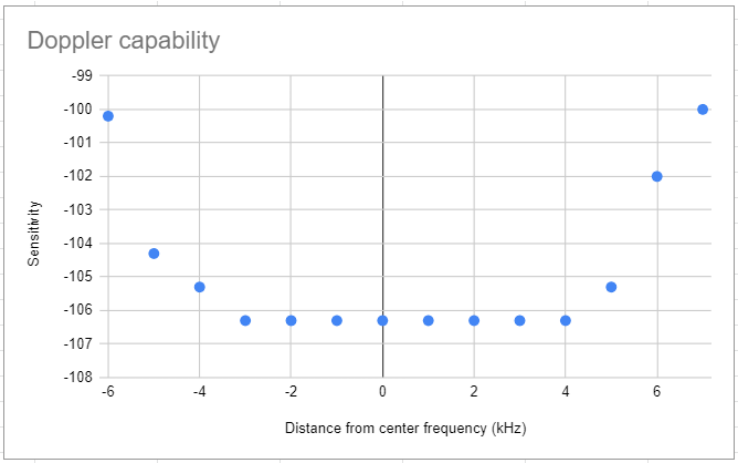

Figure 45: Test results for the doppler capability test. The transmission power was decreased at every frequency until the BER grew larger than 10^{-4}, and this was defined as the sensitivity. The receiver works well in a 10 kHz band.

4.11 Adjacent channel selectivity and saturation of adjacent channel

This test shows how a transmission in the adjacent channel effects the reception of transmission. The test requires a second transmitter, which is set to transmit CW mode at the adjacent channel, 50 kHz above or below the 437.125 MHz frequency. The power level for this transmission is given as −50 dBm by the ETSI standard, while the actual transmission power level is set to 3 dB above the sensitivity limit. Attempting to perform the test with the values given by the ETSI standard results in the noise floor rising above the transmission power level drowning out any possibility to detect the transmitted signal. Lowering the transmission power at adjacent channel to about −60 dBm lowers the noise floor enough for the signal to be once again detected. The main thing to take away from this test is that when there's a strong transmitter at the adjacent channel near the satellite, such as another satellite, it will most likely drown out any ground station transmission beneath the generated noise. Thankfully it is highly unlikely that a satellite will spend a long period of time nearby a satellite operating at the adjacent channel. However it could become an issue if the amateur radio bands get more crowded, especially if isotropic antennas are generally used.

4.12 Behaviour at high wanted signal levels

High signal levels could cause a receiver to saturate, causing problems with signal reception. This is most likely not an issue with satellites. However if a ground station is used for long range testing on the ground, it could overdrive the low noise amplifier. Similarly any transmission from a neighbouring satellite soon after deployment could cause high power levels at the input of the radio. Testing higher powers is unnecessary as the source of such a signal could likely only be another satellite very close by, and the odds of that happening are small.

The Foresail-1 COM subsystem was subjected to a transmission signal level of −30 dBm which it was able to receive without an issue. The measurement setup was similar to the sensitivity testing, but some attenuation was removed to reach higher power levels.

4.13 Environmental testing

The communications subsystem has gone through thermal vacuum testing and vibration testing during the qualification test campaign. The COM has been running after both test types and is confirmed to operate equally to before undergoing the test benches.

The COM subsystem did not undergo specific functional test procedures after the environmental testing, but the sensitivity and transmission parameters have been undergoing tests on multiple occasions after the vibration tests.

Additional thermal vacuum testing is planned and could show a problem with the power amplifier due to thermal issues. The amplifier dissipates up to 3 Watts of

power, if the according to power measurements. Any convection through air could help prevent overheating, whereas in vacuum the heating could result in damage of the power amplifier or the components around it. The power amplifier however has good thermal conductivity to the ground planes through multiple vias. The ground plane is then working as a cooler for the power amplifier. Conducting heat away from this ground plane is the main reason the ambient air works well as coolant. The only way the heat can be dissipated when the satellite is in a vacuum is by conduction through the connectors and mounting holes and radiation. An attempt to increase heat dissipation through radiation is done by anodizing the aluminium structural wall above the Foresail-1 COM subsystem black.

In addition to passively controlling the temperature, the temperature sensors are used to detect possible overheating issues. If a set threshold temperature limit is reached, the transmission power and time can be limited.

4.14 Additional testbenches

The test benches described in this chapter have confirmed the functionality of the COM subsystem to a level that fulfills the requirements. However the receive sensitivity and transmission efficiency are something that could be further improved. The sensitivity of $-106\,\mathrm{dBm}$ and transmit efficiency of $26\,\%$ are lower than the theoretical sensitivity calculated in Chapter 2 by about $8\,\mathrm{dB}$ and the transmit efficiency of the RF5110G PA of over $50\,\%$.

Additional test benches will include the previously mentioned thermal vacuum test with transmission on, and visual inspection of soldering with the help of an X-ray machine.

Testing with antenna implementation and protocol will be performed in a long-range test bench in a campaign to verify the complete satellite functions as an integrated system.

5 Conclusions

With the growing number of nanosatellites going to Earth orbits, it becomes more important to ensure that the microwave spectrum is used responsibly. This means that nanosatellite developers need to make sure their radio devices perform in accordance to international rules. Additionally, nanosatellites have been shown to suffer from poor reliability. A large portion of the failures have been estimated to come out of the communications subsystem failures. [43]

To build a functioning and reliable communications subsystem, multiple aspects have to be considered. This thesis shows the steps taken to improve and test the functionality of the Foresail-1 CubeSat communications subsystem, which will be operating in the amateur radio UHF band.

Chapter 2 explored methods for testing communications subsystems, documented by other CubeSat projects. Also, applicable regulations and standards were used to create a set of test benches that could be useful or necessary. Also, this chapter introduced theoretical aspects behind microwave communication and circuitry that would be useful in creating a link budget or when matching circuits.

In Chapter 3, the communications subsystem radio frequency chain portions were simulated with circuit simulators and EM simulators in order to choose the correct values for the lumped element components. This included the radio frequency component matching circuits and filters. The simulated values were then implemented onto a circuit board and measured with a vector network analyzer. All filters and matching circuits showed promising results, and with iterative tuning the filters were working in the desired frequencies. The matching circuit of the power amplifier showed an impedance close to the required load impedance.

In Chapter 4 applicable test benches for the Foresail-1 COM subsystem was generated. Tests for the power output, efficiency, receive sensitivity and transmit spectrum were performed. The power output of the transmission was above 30 dBm, which is within the system requirements. The sensitivity was -106 dBm, which is enough for about 4 dBm margin in the uplink budget. The spectrum of the transmission was within the emission masks set by ETSI in almost every measurement point. At a few kHz distance from the occupied band, the mask was exceeded by about 4 dB. There were no harmonic emissions visible in the spurious domain. The efficiency of the power amplifier was not optimal and warrants further investigation.

5.1 Future Work

Further testing and improved methods for PA matching are needed. Further tests mentioned in Chapter 4, to improve the performance of the Foresail-1 COM system shall be incorporated to future test benches.

Additional test benches for example for the calibration of onboard telemetry, testing the satellite in active state in a thermal vacuum and long range full functionality tests should be explored.

References

[1] Suhila Abulgasem et al. "Antenna Designs for CubeSats: A Review". In: *IEEE Access* 9 (2021), pp. 45289–45324.

[2] Alicia Johnstone. *CubeSat Design Specification Rev. 14*. en. Design Specification ETSI EN 300 220-1 V3.1.1 (2017-02). San Louis Obispo, California: The CubeSat Program, 2020. URL: https://www.cubesat.org/.

[3] *AS193-73, AS193-73LF: PHEMT GaAs IC High-Linearity 3 V Control SPDT Switch 0.1–2.5 GHz, rev. C*. AS193-73. SKYWORKS. July 2006.

[4] Dominik Barbarić, Josip Vuković, and Dubravko Babic. "Link budget analysis for a proposed Cubesat Earth observation mission". In: *2018 41st International Convention on Information and Communication Technology, Electronics and Microelectronics (MIPRO)*. IEEE. 2018, pp. 0133–0138.

[5] Ivan M. Bland. "Receive Sensitivity Characterization of the PolySat Satellite Communication System". English. Master's thesis. California Polytechnic State University, San Luis Obispo, 2010, pp. 129 + 15. URL: https://doi.org/10.15368/theses.2010.34.

[6] *CC1125 Ultra-High Performance RF Narrowband Transceiver, rev. E*. Datasheet. Texas Instruments. Oct. 2014.

[7] D.K. Cheng. *Field and Wave Electromagnetics*. Addison-Wesley series in electrical engineering. Addison-Wesley, 1989. ISBN: 9780201128192. URL: https://books.google.fi/books?id=KL%5C_vAAAAMAAJ.

[8] Commission for Communication Regulation. *ITU Emission designators*. https://www.comreg.ie/media/dlm_uploads/2015/12/ComReg0834.pdf. Accessed: 2021-11-19.

[9] *Communications PULSAR-TMTC*. AAC Clyde Space. July 2020.

[10] L.W. Couch. *Digital and Analog Communication Systems*. Always Learning. Pearson, 2012. ISBN: 9780273774211. URL: https://books.google.fi/books?id=tVSougAACAAJ.

[11] *Cubesat Communication Systems: 2003-2018*. https://www.klofas.com/comm-table/table.pdf. Accessed: 2021-11-18.

[12] *DATASHEET UHF Transceiver, datasheet*. EnduroSat. Apr. 2021.

[13] *DATASHEET X-Band Transmitter, datasheet*. EnduroSat. May 2021.

[14] Zachary Scott Decker. "A systems-engineering assessment of multiple CubeSat build approaches". PhD thesis. Massachusetts Institute of Technology, 2016, pp. 98+3. URL: http://hdl.handle.net/1721.1/105560.

[15] Gregory F Dubos, Jean-Francois Castet, and Joseph H Saleh. "Statistical reliability analysis of satellites by mass category: Does spacecraft size matter?" In: *Acta Astronautica* 67.5-6 (2010), pp. 584–595.

[16] *Tailored ECSS Engineering Standards for In-Orbit Demonstration CubeSat Projects*. Standard. Noordwijk, The Netherlands: European Cooperation for Space Standardisation, Mar. 2000.

[17] *Space Engineering, Testing*. Standard. Noordwijk, The Netherlands: European Cooperation for Space Standardization - ECSS Secretariat, June 2012.

[18] *Space engineering - Electrical and electronic*. Standard. Noordwijk, The Netherlands: European Cooperation for Space Standardization - ECSS Secretariat, July 2008.

[19] *Space engineering, Radio frequency and modulation*. Standard. Noordwijk, The Netherlands: European Cooperation for Space Standardization - ECSS Secretariat, Oct. 2011.

[20] *Space engineering, Communications*. Standard. Noordwijk, The Netherlands: European Cooperation for Space Standardization - ECSS Secretariat, July 2008.

[21] European Telecommunications Standards Institute. *Short Range Devices (SRD) operating in the frequency range 25 MHz to 1 000 MHz; Part 1: Technical characteristics and methods of measurement*. en. Standard ETSI EN 300 220-1 V3.1.1 (2017-02). Sofia Antipolis Cedex, France: European Telecommunications Standards Institute, 2017. URL: https://www.etsi.org/deliver/etsi_en/300200_300299/30022001/03.01.01_60/en_30022001v030101p.pdf.

[22] Niemela P. Forsten H. *Aalto-1 Design of UHF Transceiver*. A1-COM-DD-01-v1. Aalto University, School of Electrical Engineering. 2015.

[23] P. Fortescue, G. Swinerd, and J. Stark. *Spacecraft Systems Engineering*. Aerospace Series. Wiley, 2011. ISBN: 9780470750124.

[24] Craig Francis. "ISM S-Band CubeSat Radio designed for the PolySat System Board". English. Master's thesis. California Polytechnic State University, San Luis Obispo, 2016, pp. 183 + 11. URL: https://doi.org/10.15368/theses.2016.32.

[25] G Garcia-Cuadrado. "Nanosatellites-The Tool for a New Economy of Space: Opening Space Frontiers to a Wider Audience". In: *Journal of Aeronautics & Aerospace Engineering* 6.2 (2017), pp. 1–11.

[26] A.R. Harish and M. Sachidananda. *Antennas and Wave Propagation*. Oxford higher education Antennas and wave propagation. Oxford University Press, 2007. ISBN: 9780195686661.

[27] E. Hirvonen. *Foresail-1 Antenna Simulations*. Aalto University, School of Electrical Engineering. 2021.

[28] *IARU Amateur Satellite Frequency Coordination - list of satellite projects for which frequencies have been coordinated*. http://www.amsatuk.me.uk/iaru/finished.php. Accessed: 2021-11-15.

[29] *IARU Amateur satellites Wiki*. https://www.iaru-r1.org/wiki/Amateur_satellites. Accessed: 2021-11-19.

[30] Texas Instruments. *SmartRF Studio*. https://www.ti.com/tool/SMARTRFTM-STUDIO. Accessed: 2021-11-21.

[31] *ISISPACE VHF uplink/UHF downlink Full Duplex Transceiver*. https://www.isispace.nl/product/isis-uhf-downlink-vhf-uplink-full-duplex-transceiver/. Accessed: 2021-11-19.

[32] *ITU Radio Regulations*. Regulation. Geneva: International Telecommunication Union.

[33] *Characteristics, definitions and spectrum requirements of nanosatellites and picosatellites, as well as systems composed of such satellites*. Report. Geneva: International Telecommunication Union, Sept. 2014.

[34] *Current practices and procedures for notifying space networks currently applicaple to nanosatellites and picosatellites*. Report. Geneva: International Telecommunication Union, May 2015.

[35] *Technical characteristics for telemetry, tracking and command in the space operation service below 1 GHz for non-GSO satellites with short duration missions*. Report. Geneva: International Telecommunication Union, Sept. 2018.

[36] *Unwanted emissions in the out-of-band domain*. Recommendation. Geneva: International Telecommunication Union, Aug. 2015.

[37] *Unwanted emissions in the spurious domain*. Recommendation. Geneva: International Telecommunication Union, Sept. 2012.

[38] *Necessary bandwidth*. Recommendation. Geneva: International Telecommunication Union, Oct. 1997.

[39] *ITU-R: Managing the radio frequency spectrum for the world*. https://www.itu.int/en/mediacentre/backgrounders/Pages/itu-r-managing-the-radio-frequency-spectrum-for-the-world.aspx. Accessed: 2021-11-18.

[40] Stephen A Jacklin. "Small-satellite mission failure rates". In: *NASA/TM—2018–220034* (2019).

[41] Erik Kulu. *Nanosats Database*. https://www.nanosats.eu. Accessed: 2021-11-15.

[42] Urmas Kvell. "ESTCube-1 satellite beacon". English. Master's thesis. University of Tartu. Faculty of science and technology, Institute of Physics, 2010, p. 71. URL: http://hdl.handle.net/10062/25582.

[43] M Langer and J Bouwmeester. "Reliability of CubeSats-Statistical Data, Developers' Beliefs and the Way Forward, AIAA". In: *USU Conference on Small Satellites*. 2016.

[44] Kyle Leveque et al. "Unlocking the next generation of nano-satellite missions with 320 Mbps Ka-band downlink: On-orbit results". In: (2019).

[45] *LNA Tuned for the 433.05MHz to 434.79MHz European ISM Band, Application note*. Maxim Integrated. Sept. 2002.

[46] *MAX2640/MAX2641 300MHz to 2500MHz SiGe Ultra-Low-Noise Amplifier, rev. 4*. MAX2640. Maxim Integrated. Feb. 2015.

[47] Janet Golio Mike Golio. *RF and Microwave Circuits, Measurements, and Modeling (1st ed.)* Oxford higher education Antennas and wave propagation. CRC Press, 2007. ISBN: 9781315221878.

[48] NanoAvionics. *CubeSat UHF Digital Radio Transceiver SatCOM UHF*. https://nanoavionics.com/cubesat-components/cubesat-uhf-digital-radio-transceiver-satcom-uhf/. Accessed: 2021-11-19.

[49] P. Niemelä. *FS1 Interface Control Sheet*. Aalto University, School of Electrical Engineering. 2021.

[50] Cristóbal Nieto-Peroy and M Reza Emami. "CubeSat mission: From design to operation". In: *Applied Sciences* 9.15 (2019), p. 3110.

[51] Martin von der Ohe. "Small satellite TT&C allocations below 1 GHz: outcome of ITU WRC-19". In: *CEAS Space Journal* 12.4 (2020), pp. 565–571.

[52] M Palmroth et al. "FORESAIL-1 CubeSat Mission to measure radiation belt losses and demonstrate deorbiting". In: *Journal of Geophysical Research: Space Physics* 124.7 (2019), pp. 5783–5799.

[53] David M. Pozar. "Microwave engineering education: From field theory to circuit theory". In: *2012 IEEE/MTT-S International Microwave Symposium Digest*. 2012, pp. 1–3. DOI: 10.1109/MWSYM.2012.6259373.

[54] *Quartz crystal*. ABM8W. ABRACON. Sept. 2018.

[55] *RF5110G 3V General Purpose/GSM Power Amplifier, rev. F*. RF5110G. Qorvo. Dec. 2020.

[56] Luca Rugini and Giuseppe Baruffa. "BER of nonorthogonal FSK for IEEE 802.15. 4". In: *2018 IEEE 29th Annual International Symposium on Personal, Indoor and Mobile Radio Communications (PIMRC)*. IEEE. 2018, pp. 570–571.

[57] Md Samsuzzaman et al. "BIRDS-1 CubeSat constellation using compact UHF patch antenna". In: *IEEE Access* 6 (2018), pp. 54282–54294.

[58] S.R. Saunders and A. Aragón-Zavala. *Antennas and Propagation for Wireless Communication Systems*. Wiley, 2007. ISBN: 9780470848791.

[59] Bernard. Sklar. *Digital communications : fundamentals and applications*. eng. Upper Saddle River (NJ), 2001.

[60] Francisco Solano Eizaguirre. "S-band transmitter design for radar applications, GaN based." English. Master's thesis. Aalto University. School of Electrical Engineering, 2016, pp. 80+7. URL: http://urn.fi/URN:NBN:fi:aalto-201611025395.

[61] *SSA3000X Plus Spectrum Analyzer, datasheet, DS0703P_E02A*. SSA3021X Plus. Siglent.

[62] Qucs team. *Quite Universal Circuit Simulator*. http://qucs.sourceforge.net/. Accessed: 2021-11-22.

[63] B Tiseo et al. “Tailoring of ECSS Standard for Space Qualification Test of CubeSat Nano-Satellite”. In: *International Journal of Aerospace and Mechanical Engineering* 13.4 (2019), pp. 295–302.

[64] Armen Toorian, Ken Diaz, and Simon Lee. “The cubesat approach to space access”. In: *2008 IEEE Aerospace Conference*. IEEE. 2008, pp. 1–14.

[65] *TRAFICOM - Satelliittijärjestelmien radiolähettimet*. https://www.traficom.fi/fi/viestinta/viestintaverkot/satelliittijarjestelmien-radiolahettimet. Accessed: 2021-11-19.

[66] Thierry Turletti. “GMSK in a nutshell”. In: *Telemedia Networks and Systems Group LCS, MIT-TR* (1996).

[67] *UHF Transceiver Type II, User manual, rev. 1.5*. EnduroSat. Nov. 2018.

[68] International Telecommunications Union. *ITU Small Satellite Handbook*. Working Document on Developing an ITU-R Small Satellite $HB_W P4A$. Accessed: 2021-11-19, rev, Document 4A/TEMP/208.

[69] The International Amateur Radio Union. *Frequency coordination agreement*. Hans Blondeel Timmerman, IARU Satellite Advisor’. Dec. 2018.

[70] Sarah Walsh et al. “Development of the EIRSAT-1 CubeSat through Functional Verification of the Engineering Qualification Model”. In: *Aerospace* 8.9 (2021), p. 254.

[71] Austin Williams. “A Compact, Reconfigurable UHF Communication System Design for use with PolySat’s Embedded Linux Platform”. English. Master’s thesis. California Polytechnic State University, San Luis Obispo, 2013, pp. 92 + 12. URL: https://doi.org/10.15368/theses.2013.173.

[72] Yen Wong et al. “NASA Near Earth Network (NEN) DVB-S2 Demonstration Testing for Enhancing Higher Data Rates for CubeSat/Small Satellite Missions at X-band and Ka-band”. In: (2020).